



# EUROPEAN MECHANICAL SCIENCE

2017

VOLUME

01

ISSUE

02



Editor in Chief: M. Ozcanli

## Editorial Board

### Editor in Chief

Mustafa Ozcanli

### Editors

Besir Sahin

Hasan Serin

M. Atakan Akar

Ahmet Calik

Tayfun Ozgur

### Layout Editor

Ahmet Calik

### Secretary

Safak Yildizhan

### Revivers of this issue

Erinc Uludamar	Mehmet Bilgili
Alper Yilmaz	Arif Ozbek
Ahmet Calik	Hasan Serin
Mustafa Ozcanli	Erdi Tosun
Ertac Hurdogan	Durmus Ali Bircan
Gökhan Tüccar	Sefa Yıldırım

## Contents

<b>Editorial Board</b>	<b>1</b>
<b>Non-Destructive examination of underground pressure vessels using acoustic emission (AE) techniques<sup>s</sup></b>	<b>1</b>
Deniz Karaduman <sup>1</sup> , Durmuş Ali Bircan <sup>2</sup> , Ahmet Çetin <sup>3</sup>	
<b>Analysis of dehumidification and humidity removal process of desiccant wheel<sup>s</sup></b>	<b>9</b>
Osman Kara <sup>1</sup> , Ertaç Hürdoğan <sup>2</sup> , Orhan Büyükalaca <sup>3</sup>	
<b>Comparative analysis of various modelling techniques for emission prediction of diesel engine fueled by diesel fuel with nanoparticle additives<sup>s</sup></b>	<b>15</b>
Erdi Tosun <sup>1*</sup> , Tayfun Ozgur <sup>2</sup> , Ceyla Ozgur <sup>2</sup> , Mustafa Ozcanli <sup>2</sup> , Hasan Serin <sup>2</sup> , Kadir Aydin <sup>2</sup>	
<b>The lateral inhibition as conditional entropy enhancer<sup>s</sup></b>	<b>24</b>
Sefa Yıldırım <sup>1*</sup> , Zulfiye Arikan <sup>2</sup> , Serhan Ozdemir <sup>2</sup>	
<b>Pulsating flow and heat transfer in wavy channel with zero degree phase shift<sup>s</sup></b>	<b>31</b>
Harun Zontul <sup>1*</sup> , Nazım Kurtulmuş <sup>2</sup> , Beşir Şahin <sup>3</sup>	

# Influence of the compression ratio on the performance and emission characteristics of a vcr diesel engine fuelled with alcohol blended fuels<sup>§</sup>

Hasan Serin<sup>1\*</sup>, Şafak Yıldızhan<sup>2</sup>

<sup>1,2</sup>Department of Automotive Engineering, Çukurova University, Turkey

## Abstract

The present study is an experimental study that investigates the performance and emission characteristics of a variable compression ratio (VCR) diesel engine when the engine is fuelled with diesel, biodiesel, and small amount of alcohol blended fuels. The experimental study was evaluated with a single cylinder, water cooled, multi fuel VCR diesel test engine. The experimental results showed that increasing compression ratio improves performance characteristics such as brake thermal efficiency and specific fuel consumption of the test engine for all test fuels. However, increasing compression ratio caused to increase of NO<sub>x</sub> and CO<sub>2</sub> emissions. Blending alcohol with diesel fuel showed a slight decrement in the means of brake thermal efficiency and thus elevated specific fuel consumption values. The maximum increment of specific fuel consumption was measured as 0,34% for diesel-alcohol blends. But, blending alcohols with biodiesel fuel improved performance characteristics of the engine compared to diesel fuel up to 2,65%. Blending biodiesel with alcohols showed improvement in the means of NO<sub>x</sub> emissions up to 6,01%.

**Keywords:** Compression ratio, Alcohol, Biodiesel, Performance, Emission.

## 1. INTRODUCTION

The high cost and the hazard of the running out of fossil fuels, also the narrowing range of environmental legislations force researchers to investigate more eco-friendly, low cost and renewable energy sources [1, 2]. Biofuel usage is increasing day by day tremendously. The advantages of biofuels such as being renewable and biodegradable make biofuels more favourable compared to fossil fuel. However, biofuels have some drawbacks such as lower energy density and higher cost presently [3-5].

Biodiesel is one of the promising biofuels which is widely used and has been investigated by many researchers. Biodiesel has many advantages such as high oxygen content and being absence of sulphur, besides the having the advantages of being biofuel. But in contrary, biodiesel usage causes to increase of NO<sub>x</sub> emissions and slightly increases specific fuel consumption [6-8]. One of the biofuel alternatives is alcohol usage as energy source. Alcohols (methanol, ethanol, butanol, propyl alcohol etc.) seem to be a good alternative for spark ignition engines and a promising additive for diesel engines. Alcohols are mostly produced by fermentation and distillation of corns and sugar canes, and starch crops. Also, wood, garbage, biomass, natural gas and coal can be used for alcohol production with different methods [9].

Alcohols such as methanol and ethanol has the advantage of high octane rating, extra oxygen content, and lower carbon-hydrogen ratio compared to fossil based fuels. Alcohol usage as additive for biodiesel can improve the one of the most significant drawbacks of biodiesel usage which is relatively very higher rate of NO<sub>x</sub> emission caused by higher combustion temperature of biodiesels. Alcohols have high vaporization heat which cools the air introducing the cylinder and thus decrease the end-cylinder temperature. Also cooling effect of the alcohol improves the volumetric efficiency of the engine and provides better brake thermal efficiency [10-12].

Several investigations have been made by many researchers on the use of alcohols as fuel additives in spark ignition and compression ignition engines [13-16]. Tosun et al., (2014) investigated the effects of different alcohols such as methanol, ethanol, and butanol on the performance and emission characteristics of a diesel engine when the alcohols are blended with peanut biodiesel [7]. The study showed that, alcohol addition to peanut methyl ester improved performance and combustion characteristics of the engine compared to peanut methyl ester. According to study, alcohol-biodiesel blends showed up to 20,53% reduction in the means of the CO emissions. Lattimore et al., (2016) investigated the effects of

\*Corresponding author

Email: hserin@cu.edu.tr (H. Serin)

<sup>§</sup> This paper was presented in the IMSEC-2016

compression ratio and fuel characteristics on combustion and particulate matter emissions in a single cylinder gasoline engine [17]. The authors revealed that, addition ethanol or butanol decreases the combustion duration. The study also showed that, blending gasoline with butanol improves particulate matter and blending with ethanol improves NOx emissions.

## 2. MATERIAL AND METHOD

### 2.1 Experimental Fuels

The experimental study was conducted in Petroleum Research and Automotive Engineering Laboratories of the Department of Automotive Engineering at Çukurova University. False flax oil (Camelina Sativa) was used as raw material for biodiesel production. False flax methyl ester (FFME) was produced via the transesterification method. The reaction was performed with methyl alcohol in the presence of a catalyst (NaOH). The metoxide was obtained before the reaction by reaction methyl alcohol and NaOH. The reaction was evaluated in a spherical glass reactor equipped with reflux condenser, stirrer and thermometer. The reaction were performed with, methanol 20 wt %, sodium hydroxide 0.5 wt %. After the obtaining metoxide, the crude false flax samples and metoxide were mixed in the reactor. The mixture was heated up to 65°C and kept at this temperature for 90 minutes by stirring. After the reaction period, the crude methyl ester was waited at separating funnel for 8 hours. And then, crude glycerine was separated from methyl ester. Finally, the crude methyl ester was washed by warm water until the washed water became clear and dried at 105 °C for 1 hour. Finally washed and dried methyl ester was passed through a filter. At the end of the transesterification reaction 97% conversion of oil was obtained. Flow diagram of biodiesel production process is shown in Figure 1.



Figure 1: Biodiesel production flow diagram

Table 1 Test fuels

Fuel	Composition	Test Fuel
Low Sulphur Diesel	100% Diesel	D
False Flax Biodiesel	100% FFME	B
Diesel-Methanol	95% Diesel + 5% Methanol	DM
Diesel-Ethanol	95% Diesel + 5% Ethanol	DE
Diesel-Butanol	95% Diesel + 5% Butanol	DBu
Biodiesel-Methanol	95% FFME + 5% Methanol	BM
Biodiesel -Ethanol	95% FFME + 5% Ethanol	BE
Biodiesel -Butanol	95% FFME + 5% Butanol	BBu

In the study, low sulphur diesel fuel (conventional diesel), false flax biodiesel (false flax methyl ester), diesel-alcohol, and biodiesel-alcohol blends were investigated in the means of performance and emission characteristics. In the study, three different alcohols which are Methanol (CH<sub>3</sub>OH), Ethanol (C<sub>2</sub>H<sub>5</sub>OH), and Butanol (C<sub>4</sub>H<sub>9</sub>OH) were used. The alcohols were blended with diesel fuel and biodiesel fuel. The test fuels were given in Table 1. Also some psychical properties of alcohols used in the study were given in Table 2.

Table 2 Psychical properties of alcohols used in the study

Specification	Unit	Methanol (CH <sub>3</sub> OH)	Ethanol (C <sub>2</sub> H <sub>5</sub> OH)	Butanol (C <sub>4</sub> H <sub>9</sub> OH)
Purity (GC)	%	>=99,8	>=99,0	>=99,8
Density (20 oC)	gr/cm <sup>3</sup>	0,791-0,793	0,791-0,793	0,810
Melting Point	oC	-97,6	-116	-89
Viscosity Dynamical (20 oC)	m.Pa.s	0,545	1,2	2,57
Molar Mass	gr/mol	32,04	32,04	74,12
Water	(K.F.)	<=0,1	<=0,5	<=0,5

The psychical properties of the test fuels were measured before testing them in the test engine. Instruments used for analysing the products were; Zeltex ZX 440 NIR petroleum analyser with an accuracy of ±0.5 for determining cetane

number; Tanaka AFP-102 for cold filter plugging point; Tanaka AKV-202 Auto Kinematic Viscosity test for determining the viscosity; Kyoto electronics DA-130 for density measurement, Tanaka flash point control unit FC-7 for flash point determination and IKA Werke C2000 bomb calorimeter for determination of heating value. The fuel quality measurements were performed according to EN 14214 and EN 590.

## 2.2 Test Rig

In the study, a single cylinder, water cooled, multi fuel, variable compression ratio (VCR) diesel engine and an eddy current dynamometer was used in order to evaluate the performance and emission characteristics of the fuels. All of the experiments were conducted under partial load (60%) conditions due to full load operating conditions deteriorate the accuracy of the experiments since the too vibrant operating of the single cylinder engines. The experiments were evaluated at three different compression ratios (12:1, 14:1 and 16:1). Before the experiments the test engine was run for 15 minutes to achieve the stable operating conditions. The exhaust emission characteristics of the engine were also measured simultaneously. Table 3 and 4 shows the technical specifications of the engine test rig and the exhaust emission measurement device. Figure 2 demonstrates the schematic representation of experimental procedure.

Table 3 Technical specifications of the test engine and emission device

Brand	Kirloskar Oil Engines	Brand	MRU Air Delta 1600 V
Model	240	CO	0-10%
Configuration	Single Cylinder	CO <sub>2</sub>	0-20%
Type	Four Stroke, Water Cooled	HC	0-20000 ppm
Displacement	661 cc	O <sub>2</sub>	0-22%
Bore	87.5 mm	NO	0-4000 ppm
Stroke	110 mm	NO <sub>2</sub>	0-1000 ppm
Maximum/Minimum Operating Speed	2000/1200 rpm	Lambda	0-9.99
Power	3.5 Kw @ 1500 rpm	Accuracy	According to OIML-class 1
CR range	12:1-18:1	Ambient Temperature	+5o - +45 oC
Injection Variation	0-25 Deg BTDC	Exhaust Gas Temperature	Max 650 oC
Peak Pressure	77.5 kg/cm <sup>2</sup>		
Air cleaner	Paper element type		
Weight	160 kg		
Combustion Principle	Compression Ignition		
Lubricating System	Forced Feed System		

## 3. RESULTS AND DISCUSSIONS

### 3.1 Fuel Properties

Fuel properties of low sulphur diesel, false flax oil methyl ester, and their blends with various alcohols were given in table 4. It can be seen from the fuel property test results diesel and biodiesel fuels used in the study were within the diesel and biodiesel standards. Alcohol addition to both diesel and biodiesel fuels decreased slightly the density values due to lower density of alcohols. Also, lower heating values of diesel-alcohol and biodiesel-alcohol blends were lower than diesel and biodiesel fuels. Blending alcohol resulted in with lower viscosity which can cause fuel pump plugs for both diesel and biodiesel fuels. Since the blend ratio was a small amount, psychical properties of test fuels were not significantly different compared to diesel and biodiesel fuels.

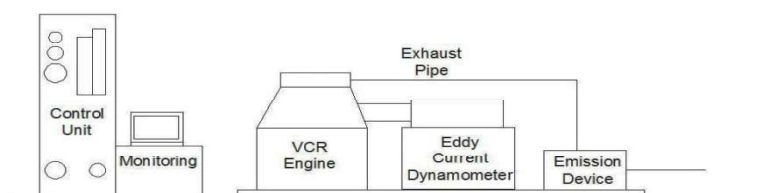


Figure 2: Schematic representation of the experimental test rig

Table 4 Fuel properties of test fuels

Fuel Properties	Test Fuels									
	D	EN590	B	EN 14214	DM	DE	DBu	BM	BE	BBu
Density (20 oC) kg/m <sup>3</sup>	837	820-845	883	860-900	831	832	834	879	879	880
Cetane Number	59,47	Min 51	51,62	Min 51	56,5	57,2	58,1	49,45	50,16	50,75
CFPP oC	-11	-	-8	Summer<4 Winter<1	-11	-11	-12	-8	-8	-10
Heating Value, MJ/kg	45.-,85	-	38,22	-	44,55	44,99	45,21	37,29	37,74	37,96
Kinematic Viscosity (40 oC) mm <sup>2</sup> /s	2,76	2,0-4,5	4,29	3.5-5.0	2,68	2,71	2,75	4,07	4,12	4,21
Flash Point oC	79.5	Min 55	>120	Min 120	-	-	-	-	-	-

### 3.2 Performance Characteristics

Figure 3 shows the brake thermal efficiency (BTHE) results of the experiments of test fuels at different compression ratios. Brake thermal efficiency can be defined as the ratio of heat input to power output of the engine. It can be seen clearly from the graph that the increasing CR improves BTHE values of all test fuels since the higher CR improves the combustion characteristics of the engine. The experiments revealed that alcohol addition to diesel fuel slightly reduced BTHE compared to diesel fuel due to lower calorific value of the alcohols [18]. The maximum decrement of BTHE was occurred with B95M5 fuel. But, alcohol addition to biodiesel fuel improved BTHE slightly. This improvement may be due to extra oxygen content of alcohol. With the increment of compression ratio specific fuel consumption (SFC) were improved due to higher BTHE and better combustion for all test fuels [10]. Diesel-alcohol blends showed slight increment in the means of SFC (Figure 4) compared to diesel fuel. The improvement in the means of combustion at higher compression ratios showed higher exhaust gas temperature (Figure 5).

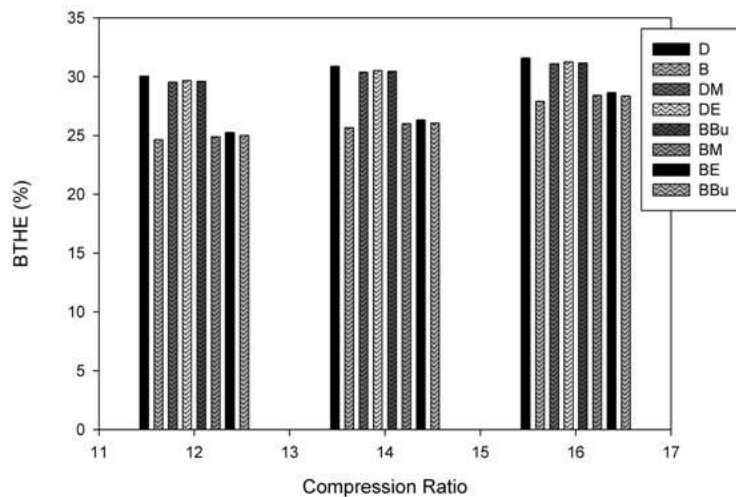


Figure 3: BTHE values of test fuels

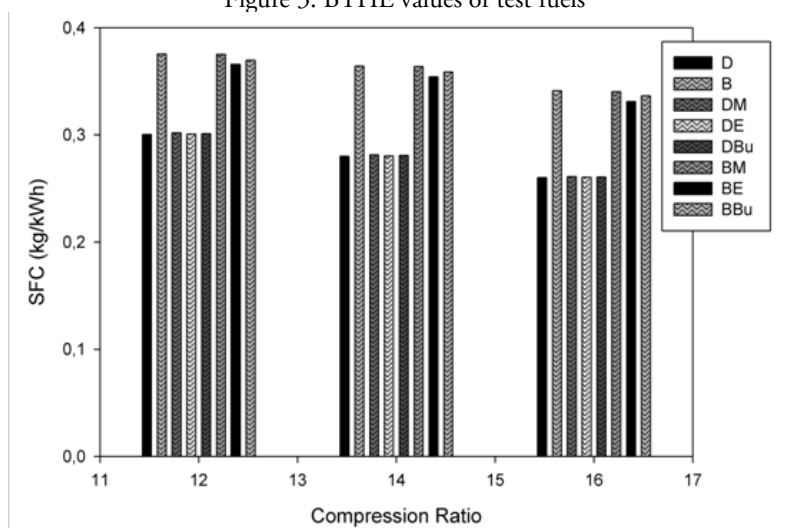


Figure 4: SFC values of test fuels

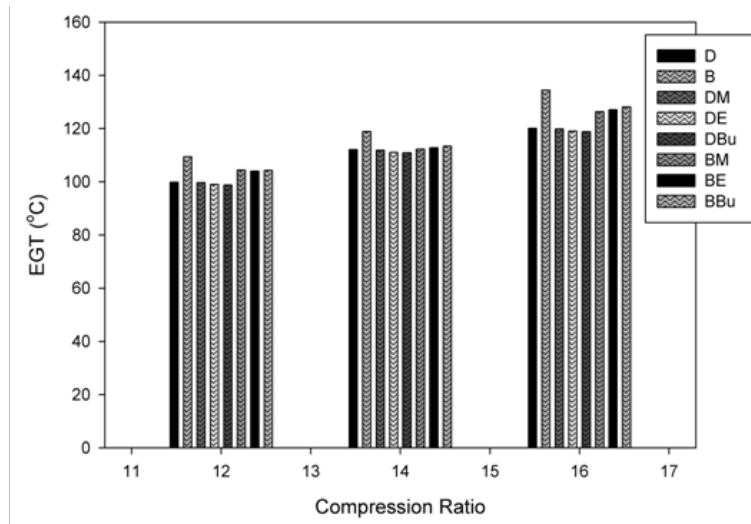


Figure 5: EGT values of test fuels

Diesel-alcohol blends showed a slight decrement in the means of BTHE and a slight increment of SFC. The maximum decrement of BTHE and the maximum increment of SFC was observed as 1,59% and 0,34% , respectively, compared to diesel fuel when the engine was fuelled with D95M5 fuel at 16:1 CR. But, blending biodiesel with alcohols showed the reverse trend of diesel-alcohol blends. The maximum improvement of BTHE for biodiesel-alcohol blends was obtained as 2,65% when B95E5 fuel used compared to biodiesel fuel. And thus, B95E5 fuel usage resulted in 2,98% improvement of SFC values.

### 3.3 Emission Characteristics

Figure 6,7,8 show the carbon monoxide (CO), carbon dioxide (CO<sub>2</sub>), and nitrogen oxides (NO<sub>x</sub>) emissions of the test fuels, respectively. The experiments revealed that increasing compression ratio decreases CO emissions due to better combustion for all test fuels but increment of compression ratio causes to increment of CO<sub>2</sub> and NO<sub>x</sub> emissions. At higher compression ratios, the more complete combustion occurs and thus, carbon molecules are mostly converted to CO<sub>2</sub> instead of CO and unburned hydrocarbons (UHC) emissions. Also, the better combustion means higher in-cylinder temperature which is the main reason of NO<sub>x</sub> formation. So, increasing CR caused to increase of NO<sub>x</sub> emissions for all test fuels.

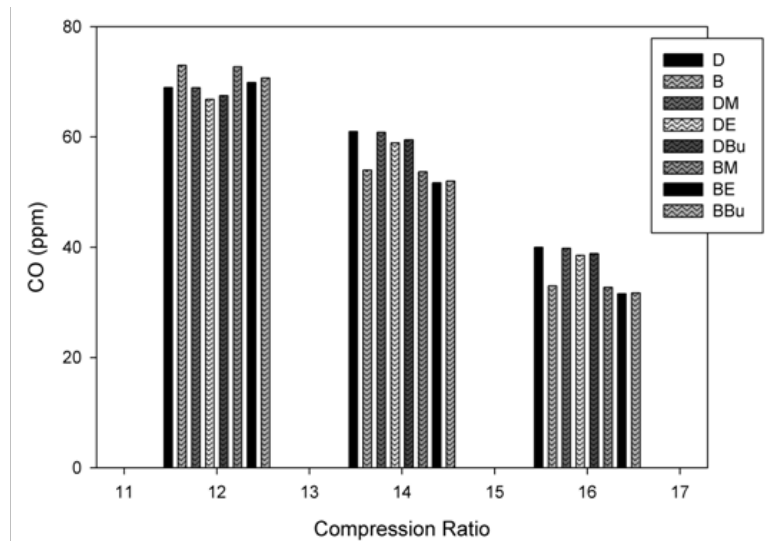


Figure 6: CO values of test fuels

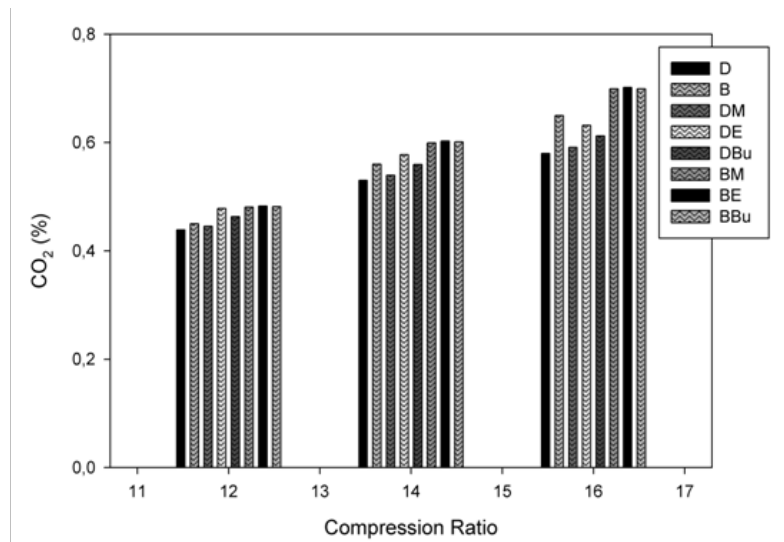


Figure 7: CO<sub>2</sub> values of test fuels

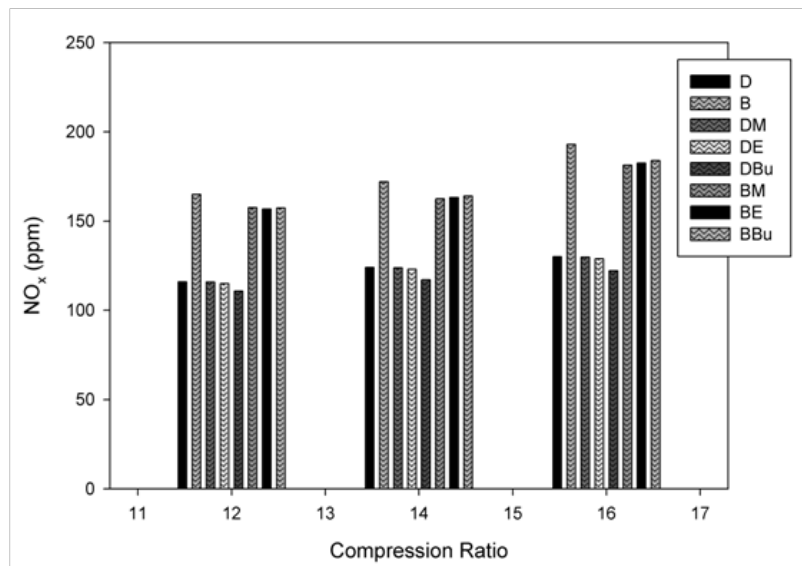


Figure 8: NO<sub>x</sub> values of test fuels

Alcohol addition to diesel fuel, improved CO emissions of diesel-alcohol blends due to extra oxygen content of alcohols compared to diesel fuel. Also, biodiesel-alcohol blends showed similar trend. The maximum decrement of CO emissions was occurred as 3,67% for diesel-alcohol blends compared to diesel fuel when engine was fuelled with D95E5 fuel at 16:1 CR. Also maximum decrement of CO emissions was measured as 3,91% for biodiesel-alcohol blends when engine was fuelled with B95Bu5 fuel compared to biodiesel fuel at 16:1 CR.

The experimental results revealed that blending diesel and biodiesel fuels with alcohols caused to increase of CO<sub>2</sub> emissions. The maximum increment of CO<sub>2</sub> emissions compared to diesel fuel was occurred as 8,97% when the engine fuelled with D95E5 fuel at 16:1 CR for diesel-alcohol blends. For biodiesel-alcohol blends, the maximum increment was observed with B95E5 fuel as 7,94% compared to biodiesel at 16:1 CR. The main reason of these trends may be due to improved combustion of diesel-alcohol and biodiesel-alcohol blends [19].

According to experimental results, blending alcohols with diesel and biodiesel fuels resulted in improved NO<sub>x</sub> emissions which are one of the main drawbacks of compression ignition engines especially when the engine is fuelled with biodiesel fuel. NO<sub>x</sub> emissions were improved for all diesel-alcohol and biodiesel-alcohol blends compared to diesel fuel and biodiesel fuel. The maximum improvement of NO<sub>x</sub> emissions for diesel-alcohol blends was obtained as 6,40% compared to diesel fuel when the engine was fuelled with D95Bu5 fuel at 16:1 CR. The maximum improvement of NO<sub>x</sub> emission for biodiesel-alcohol blends were observed when the engine was fuelled with B95M5 fuel as 6,01% compared to diesel fuel at 16:1 CR. The main reason of NO<sub>x</sub> improvements may be due to high latent heat of evaporation of alcohols which shows a cooling effect and decreases the combustion temperature. NO<sub>x</sub> formation is directly related with combustion temperature [20, 21].

## 4. CONCLUSION

In this study, performance and emission characteristics of alcohol blended fuel were evaluated. Fuel properties of the test fuels, performance and emission characteristics of the fuel at different compression ratios were studied and the following conclusions were obtained;

- BTHE and SFC values improved at higher compression ratios for all test fuels.
- Alcohol addition to diesel fuel slightly decreased BTHE and thus increased SFC.
- Alcohol addition to biodiesel fuel slightly improved BTHE and SFC values.
- Alcohol addition to both diesel and biodiesel fuels slightly improved CO emissions and caused a slight increment of CO<sub>2</sub> emissions. Also, alcohol addition improved slightly NO<sub>x</sub> emissions for both diesel and biodiesel fuels.

## 5. ACKNOWLEDGEMENTS

The authors would like to thank the Cukurova University Scientific Research Project Coordination (FBA-2016-5510) for financial support to this project.

## REFERENCES

- [1] Ozcanli, M. (2015). Castor-oil methyl ester/butanol/diesel fuel blend as an alternative for compression ignition engines. *Journal of Biotechnology*, vol. 208, p. S32. 10.1016/j.jbiotec.2015.06.089
- [2] Serin, H., Ozcanli, M., Gokce, M.K., and Tuccar, G. (2013). Biodiesel Production From Tea Seed (*Camellia Sinensis*) Oil and its Blends With Diesel Fuel. *International Journal of Green Energy*, vol. 10, no. 4, pp. 370-377. 10.1080/15435075.2012.655354
- [3] Uludamar, E., Yildizhan, Ş., Aydın, K., and Özcanlı, M. (2016). Vibration, noise and exhaust emissions analyses of an unmodified compression ignition engine fuelled with low sulphur diesel and biodiesel blends with hydrogen addition. *International Journal of Hydrogen Energy*, vol. 41, no. 26, pp. 11481-11490. 10.1016/j.ijhydene.2016.03.179
- [4] Uludamar, E. et al. (2017). Evaluation of vibration characteristics of a hydroxyl (HHO) gas generator installed diesel engine fuelled with different diesel–biodiesel blends. *International Journal of Hydrogen Energy*, <https://doi.org/10.1016/j.ijhydene.2017.01.192>
- [5] Ozcanli, M., Akar, M.A., Calik, A., and Serin, H. (2017). Using HHO (Hydroxy) and hydrogen enriched castor oil biodiesel in compression ignition engine. *International Journal of Hydrogen Energy*, 10.1016/j.ijhydene.2017.01.091
- [6] Serin, H., Ozgur, C., Ozcanli, M., Aydın, K., and Ozgur, T. (2013). Preparation of fuels by cracking of different plastics and their blends with diesel fuel. *Current Opinion in Biotechnology*, vol. 24, p. S44. 10.1016/j.copbio.2013.05.097
- [7] Tosun, E., Yilmaz, A.C., Ozcanli, M., and Aydın, K. (2014). Determination of effects of various alcohol additions into peanut methyl ester on performance and emission characteristics of a compression ignition engine. *Fuel*, vol. 126, pp. 38-43. 10.1016/j.fuel.2014.02.037
- [8] Yasin, M.H.m., Mamat, R., Yusop, A.F., Rahim, R., Aziz, A., and Shah, L.A. (2013). Fuel Physical Characteristics of Biodiesel Blend Fuels with Alcohol as Additives. *Procedia Engineering*, vol. 53, pp. 701-706. 10.1016/j.proeng.2013.02.091
- [9] Imran, A., Varman, M., Masjuki, H.H., and Kalam, M.A. (2013). Review on alcohol fumigation on diesel engine: A viable alternative dual fuel technology for satisfactory engine performance and reduction of environment concerning emission. *Renewable and Sustainable Energy Reviews*, vol. 26, pp. 739-751. 10.1016/j.rser.2013.05.070
- [10] Datta Bharadwaz, Y., Govinda Rao, B., Dharmarao, V., and Anusha, C. (2016). Improvement of biodiesel methanol blends performance in a variable compression ratio engine using response surface methodology. *Alexandria Engineering Journal*, vol. 55, no. 2, pp. 1201-1209. 10.1016/j.aej.2016.04.006
- [11] Keskin, A., Yaşar, A., Reşitoğlu, İ., Akar, M.A., and Sugözü, İ. (2013). The Influence of Diesel Fuel-biodiesel-ethanol-butanol Blends on the Performance and Emission Characteristics of a Diesel Engine. *Energy Sources, Part A: Recovery, Utilization, and Environmental Effects*, vol. 35, no. 19, pp. 1873-1881. 10.1080/15567036.2010.529568
- [12] Masum, B.M., Kalam, M.A., Masjuki, H.H., Palash, S.M., and Fattah, I.M.R. (2014). Performance and emission analysis of a multi cylinder gasoline engine operating at different alcohol–gasoline blends. *RSC Advances*, vol. 4, no. 53, pp. 27898-27904. 10.1039/c4ra04580g
- [13] Akar, M.A. (2016). Performance and emission characteristics of compression ignition engine operating with false flax biodiesel and butanol blends. *Advances in Mechanical Engineering*, vol. 8, no. 2, pp. 1-7. 10.1177/1687814016632677
- [14] Balki, M.K., Sayin, C., and Canakci, M. (2014). The effect of different alcohol fuels on the performance, emission and combustion characteristics of a gasoline engine. *Fuel*, vol. 115, pp. 901-906. 10.1016/j.fuel.2012.09.020
- [15] Imdadul, H.K. et al. (2016). Higher alcohol–biodiesel–diesel blends: An approach for improving the performance, emission, and combustion of a light-duty diesel engine. *Energy Conversion and Management*, vol. 111, pp. 174-185. 10.1016/j.enconman.2015.12.066

- [16] Tsai, J.-H. et al. (2014). Emissions from a generator fueled by blends of diesel, biodiesel, acetone, and isopropyl alcohol: Analyses of emitted PM, particulate carbon, and PAHs. *Science of The Total Environment*, vol. 466, pp. 195-202. 10.1016/j.scitotenv.2013.07.025
- [17] Lattimore, T., Herreros, J.M., Xu, H., and Shuai, S. (2016). Investigation of compression ratio and fuel effect on combustion and PM emissions in a DISI engine. *Fuel*, vol. 169, pp. 68-78. 10.1016/j.fuel.2015.10.044
- [18] Bora, B.J. and Saha, U.K. (2016). Experimental evaluation of a rice bran biodiesel – biogas run dual fuel diesel engine at varying compression ratios. *Renewable Energy*, vol. 87, pp. 782-790. 10.1016/j.renene.2015.11.002
- [19] Chavan, S.B., Kumbhar, R.R., Kumar, A., and Sharma, Y.C. (2015). Study of Biodiesel Blends on Emission and Performance Characterization of a Variable Compression Ratio Engine. *Energy & Fuels*, vol. 29, no. 7, pp. 4393-4398. 10.1021/acs.energyfuels.5b00742
- [20] Huang, Z. et al. (2005). Performance and Emissions of a Compression Ignition Engine Fueled with Diesel/Oxygenate Blends for Various Fuel Delivery Advance Angles. *Energy & Fuels*, vol. 19, no. 2, pp. 403-410. 10.1021/ef049855d
- [21] Sayin, C. and Gumus, M. (2011). Impact of compression ratio and injection parameters on the performance and emissions of a DI diesel engine fueled with biodiesel-blended diesel fuel. *Applied Thermal Engineering*, vol. 31, no. 16, pp. 3182-3188. 10.1016/j.applthermaleng.2011.05.044

# A hybrid approach for the prediction and optimization of cutting forces using grey-based fuzzy logic<sup>§</sup>

Ugur Esme\*

Mersin University/Tarsus Technology Faculty, Department of Automotive Engineering, Tarsus-Mersin

## Abstract

This study focused on the Grey-Based Fuzzy Logic Algorithm for the prediction and optimization of multiple performance characteristics of oblique turning process. Experiments have been constructed according to Taguchi's L16 orthogonal array design matrix. Cutting speed, rate of feed and depth of cut were selected as input parameters, whereas material removal rate, cutting force and surface roughness were selected as output responses. Using grey relation analysis (GRA), grey relational coefficient (GRC) and grey relation grade (GRG) were obtained. Then, Grey based fuzzy algorithm was applied to obtain grey fuzzy reasoning grade (GFRG). Analysis of variance (ANOVA) carried out to find the significance and contribution of parameters on multiple performance characteristics. Finally, confirmation test was applied at the optimum level of GFRG to validate the results. The results also show the application feasibility of the grey based fuzzy algorithm for continuous improvement in product quality in complex manufacturing processes.

**Keywords:** Turning process, cutting forces, grey relation analysis, fuzzy logic algorithm, optimization.

## 1. INTRODUCTION

Turning is a very important machining process in which a single-point cutting tool removes material from the surface of a rotating cylindrical workpiece [1]. The cutting tool is fed linearly in a direction parallel to the axis of rotation [2,3]. As indicated in Figure 1, turning is carried out on a lathe that provides the power to turn the workpiece at a given rotational speed and to feed the cutting tool at a specified rate and depth of cut. Therefore, three cutting parameters, i.e. cutting speed ( $V$ ), feed rate ( $F$ ), and depth of cut ( $D$ ), should be properly selected for better surface finish with lower cutting force [2,3].

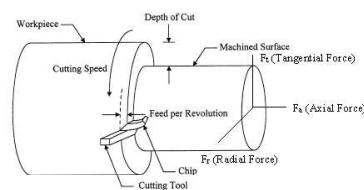


Figure 1: Schematic representation of oblique turning process [1]

In a turning operation, it is an important task to select cutting parameters for achieving high cutting performance. Usually, the desired cutting parameters are determined based on experience or by use of a handbook [1]. However, this does not ensure that the selected cutting parameters have optimal or near optimal cutting performance for a particular machine and environment. To select the cutting parameters properly, several mathematical models based on statistical regression techniques or neural computing have been constructed to establish the relationship between the cutting performance and the cutting parameters [1-8]. Then, an objective function with constraints is formulated to solve the optimal cutting parameters using optimization techniques. Therefore, considerable knowledge and experience are required for using this modern approach [1]. Furthermore, a large number of cutting experiments has to be performed and analyzed in order to build the mathematical models. Thus the required model building is very costly in terms of time and materials [1]. Basically, the grey based fuzzy logic is a powerful tool for the design of multivariable complex systems. It provides a robust systematic and efficient way in order to model the multivariable complex systems. Therefore, this study applied a Taguchi L9 orthogonal array to plan the experiments on turning process [2,3]. Three controlling factors including cutting speed ( $V$ ), depth of cut ( $d$ ) and feed rate ( $f$ ) were selected as input parameters whereas material removal rate, cutting force

\*Corresponding author

Email: [uguresme@gmail.com](mailto:uguresme@gmail.com) (U. Esme)

<sup>§</sup> This paper was presented in the IMSEC-2016

and surface roughness were selected as output responses. Using grey relation analysis (GRA), grey relational coefficient (GRC) and grey relation grade (GRG) were obtained. Then, Grey based fuzzy algorithm was applied to obtain grey fuzzy reasoning grade (GFRG). Analysis of variance (ANOVA) carried out to find the significance and contribution of parameters on multiple performance characteristics. Finally, confirmation test was applied at the optimum level of GFRG to validate the results. The results also show the application feasibility of the grey based fuzzy algorithm for continuous improvement in product quality in complex manufacturing processes [8-12].

## 2. EXPERIMENTAL PROCEDURE AND DETAILS

The cutting experiments were carried out on an experimental lathe setup using HSS cutting tool for the machining of AISI 1050 steel bar which is 30 mm in diameter and 80 mm in length. The mechanical properties and percent composition of workpiece material is listed in Table 1 [2,3].

Table 1. Chemical and mechanical properties of AISI 1050 medium carbon steel

Chemical composition %	C	P	S	Mn	Cr	Fe	Ni	Cu
	0.49	0.02	0.02	0.78	0.08	97.99	0.10	0.26
Mechanical properties	Yield strength (MPa)		Tensile strength (Mpa)		Elongation (%)		Vickers Hardness (HV)	
	365		636		24		261	

Phynix TR-100 model surface roughness tester was used to measure the surface roughness of the machined samples. Cut off length ( $\lambda$ ) was chosen as 0.3 for each roughness measurement. Average of six measurements of surface roughness was taken to use in the multi-criteria optimization. Also, material removal rate (MRR, mm<sup>3</sup>/min) was calculated using Eq. (1);

$$MRR = 1000Vfd \quad (1)$$

where  $f$  (mm/rev) denotes the feed rate,  $d$  (mm) describes the cutting depth and  $V$  (m/min) presents the cutting speed of the turning operation.

### 2.1 Process Parameters and Test Results

In full factorial design, the number of experimental runs exponentially increases as the number of factors as well as their level increases. This results huge experimentation cost and considerable time [11]. So, in order to compromise these two adverse factors and to search the optimal process condition through a limited number of experimental runs Taguchi's L9 orthogonal array consisting of 9 sets of data has been selected to optimize the multiple performance characteristics of turning process [8-12]. Experiments have been conducted with the process parameters given in Table 2, to obtain the machined surface on AISI 1050 medium carbon steel. The feasible space for the cutting parameters was defined by varying the cutting speed in the range of 110-600 m/min, the feed rate in the range of 0.2-0.6 mm/min, and the depth of cut in the range of 0.5-1.5 mm.

Table 2. Cutting parameters and their levels

Cutting Parameters	Notation	Unit	Levels of factors		
			1	2	3
cutting speed	V	m/min	110*	300	600
feed rate	f	mm/min	0.2*	0.4	0.6
depth of cut	d	mm	0.5*	1.0	1.5

\*initial factor setting

In order to prevent the sudden increase of cutting forces due to the dullness of the cutting edge, the HSS tool was changed after three repetition of each experiment. Table 3 shows the selected design matrix based on Taguchi L9 orthogonal array consisting of 9 sets of coded conditions and the experimental results for the responses of F, Ra and MRR. All these data have been utilized for analysis and evaluation of optimal parameter combination required to achieve desired quality within the experimental domain [10,11].

Table 3. Orthogonal L9 array of the experimental runs and results

Run no	Parameter level			Experimental results		
	V	f	d	MRR (mm <sup>3</sup> /min)	F (N)	R <sub>a</sub> ( $\mu$ )
1	1	1	1	0.11	123	0.87
2	1	2	2	0.44	179	2.33
3	1	3	3	0.99	364	6.62
4	2	1	2	0.60	166	1.98
5	2	2	3	1.80	295	3.82
6	2	3	1	0.90	255	3.96
7	3	1	3	1.80	340	0.92
8	3	2	1	1.20	218	1.22
9	3	3	2	3.60	268	5.60

### 3. GREY BASED FUZZY LOGIC

In this section, the constructed grey based fuzzy logic approach for oblique turning process optimization is given in details.

#### 3.1. Grey Relational Analysis (GRA)

In Grey relational analysis, experimental data i.e., measured features of quality characteristics are first normalized ranging from zero to one. This process is known as Grey relational generation. Next, based on normalized experimental data, Grey relational coefficient is calculated to represent the correlation between the desired and actual experimental data. Then overall Grey relational grade is determined by averaging the Grey relational coefficient corresponding to selected responses [13-16]. The overall performance characteristic of the multiple response process depends on the calculated Grey relational grade (GRG) [14]. This approach converts a multiple response process optimization problem into a single response optimization situation with the objective function of overall Grey relational grade. The optimal parametric combination is then evaluated which would result highest Grey relational grade. The optimal factor setting for maximizing overall Grey relational grade can be performed by Taguchi method [13,16,17]. In Grey relational generation, the normalized F and Ra corresponding to the smaller-the-better (SB) criterion which can be expressed as given in Eq. (2) [18,19]:

$$x_i(k) = \frac{\max y_i(k) - y_i(k)}{\max y_i(k) - \min y_i(k)} \quad (2)$$

MRR should follow the larger-the-better (LB) criterion, which can be expressed as given in Eq. (3) [18]:

$$x_j(k) = \frac{y_j(k) - \min y_j(k)}{\max y_j(k) - \min y_j(k)} \quad (3)$$

where  $x_i(k)$  and  $x_j(k)$  is the value after the Grey relational generation for SB and LB criterion respectively.  $\min y_i(k)$  is the smallest value of  $y_i(k)$  and for the kth response, and  $\max y_i(k)$  is the largest value of  $y_i(k)$  for the kth response [18]. An ideal sequence is  $x_0(k)$  ( $k=1,2,\dots,9$ ) for the responses. The definition of Grey relational grade in the course of Grey relational analysis is to reveal the degree of relation between the 16 sequences [ $x_0(k)$  and  $x_i(k)$ ,  $k=1,2,\dots,9$  and  $i=1,2,\dots,9$ ]. The Grey relational coefficient  $\xi_i(k)$  can be calculated as given in Eq. (4) [13,18]:

$$\xi_i(k) = \frac{\Delta_{\min} - \psi \Delta_{\max}}{\Delta_{0i}(k) + \psi \Delta_{\max}} \quad (4)$$

where  $\Delta_{0i} = \|x_0(k) - x_i(k)\|$  is difference of the absolute value  $x_0(k)$  and  $x_i(k)$ ;  $\psi$  is the distinguishing coefficient  $0 \leq \psi \leq 1$  (equal  $\psi = 0.3$  is used);  $\Delta_{\min} = \forall j^{\min} \in i \forall k^{\min} \|x_0(k) - x_j(k)\|$  is the smallest value of  $\Delta_{0i}(k)$ ; and  $\Delta_{\max} = \forall j^{\max} \in i \forall k^{\max} \|x_0(k) - x_j(k)\|$  is the largest value of  $\Delta_{0i}(k)$ . After averaging the Grey relational coefficients, the Grey relational grade  $\gamma_i$  can be computed as given in Eq. (5) [18]:

$$\gamma_i = \frac{1}{n} \sum_{k=1}^n \xi_i(k) \quad (5)$$

where n is the number of process responses. The higher value of Grey relational grade corresponds to intense relational degree between the reference sequence  $x_0(k)$  and the given sequence  $x_i(k)$ . The reference sequence  $x_0(k)$  represents

the best process sequence; therefore, higher Grey relational grade means that the corresponding parameter combination is closer to the optimal [16]. The mean response for the Grey relational grade with its grand mean and the main effect plot of Grey relational grade are very important because optimal process condition can be evaluated from this plot [18].

### 3.2 Fuzzy Inference System (FIS) Modeling

In GRA, the use of performance characteristics such as lower-the-better, higher-the-better and nominal-the-better reflects that there is some level of uncertainty in the obtained results. This uncertainty can be effectively checked by using fuzzy logic [13,19-29]. The grey-fuzzy method was created and applied by Lin in 2004 [15]. It takes a fuzzy rules approach rather than making a traditional GRG estimation for grey relational analysis. For GRG estimation, two approaches were employed to compare output performance. One is the traditional GRG function while the other is the fuzzy inference system (FIS) [13,16,28-29].



Figure 2: 3-inputs and 3-outputs fuzzy logic system

In the first step, fuzzifier uses the membership function to fuzzify inputs which are obtained before GRG calculations. Membership function is used to define how the values of the input and output are mapped to a value between 0 and 1 [14]. In the next step of the calculation, nine fuzzy rules for three inputs and one output are developed using Eq. (6) based on the results that obtained from the experiments for inference.

- Rule 1 : if X1 is A1; X2 is B1;and X3 is C1 then y is D1; else  
 Rule 2 : if X1 is A2; X2 is B2;and X3 is C2 then y is D2; else  
 ⋮  
 Rule n : if X1 is An; X2 is Bn;and X3 is Cn then y is Dn; else
- (6)
- Ai, Bi, Ci and Di are fuzzy subsets defined by the corresponding membership functions such as  $\mu_{A_i}$ ,  $\mu_{B_i}$ ,  $\mu_{C_i}$  and  $\mu_{D_i}$ .

The inference engine then performs fuzzy reasoning on fuzzy rules by taking max–min inference (Eq. (7)) to generate a fuzzy value [14].

$$\mu_{C_0}(Y) = (\mu_{A_1}(X_1) \wedge \mu_{B_1}(X_2) \wedge \mu_{C_1}(X_3) \wedge \mu_{D_1}(Y) \vee \dots \mu_{A_n}(X_1) \wedge \mu_{B_n}(X_2) \wedge \mu_{C_n}(X_3) \wedge \mu_{D_n}(Y)) \quad (7)$$

Where  $\wedge$  is the minimum operation and,  $\vee$  is the maximum operation. Finally, in this study, centroid defuzzification method was used in order to convert the fuzzified values. The centroid defuzzification method is given in Eq. (8).

$$Y_0 = \frac{\sum Y \mu_{C_0}(Y)}{\sum \mu_{C_0}(Y)} \quad (8)$$

The flowchart adopted in the present study to determine the optimal combination of ball turning parameters for the multi response optimization is shown in Figure 3.

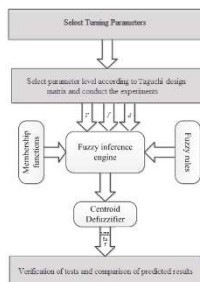


Figure 3: Flowchart of the proposed grey based fuzzy logic method

The methodology consists of a six forward step approach given below [14]:

Step 1: Selecting the Turning input parameters and their levels as given in Table 2. Perform the experiments according to the Taguchi's orthogonal design matrix given in Table 3.

Step 2: Normalize all of the responses using Eqs. (2) and (3). Calculate the grey relational coefficients using Eq. (4), and followed by calculation of grey relational grade (GRG) using Eq. (5).

Step 3: Fuzzify the grey relational coefficients obtained from each response and the overall grey relational grade using membership function. Also, establish the fuzzy rules in linguistic form relating the grey relational coefficient and the overall grey relational grade using Eq. (6).

Step 4: Using max-min interface operations given in Eq. (7), calculate the value of fuzzy multi response output (), and follow by calculating the grey-fuzzy reasoning grade  $Y_0$  using centroid defuzzification method given in Eq. (8).

Step 5: Select the optimal combination of parameters through response table and response graph obtained from grey-fuzzy optimization. Find out the contribution of each factor and their interactions on the multi response output using analysis of variance (ANOVA) Table.

Step 6: Carry out the confirmation tests to verify the results obtained and compare the results determine the improvements and percentage error.

#### 4. RESULTS AND DISCUSSION

The pre-processed data of the normalized experimental results, grey relational coefficients and the overall grey relational grade for each combination of parameters is tabulated in Table 4, Table 5 and Table 6. The grey-fuzzy reasoning grade is obtained by using MATLAB v7.10.0 (R2010a) fuzzy logic tool box.

Table 4. Grey relational generation of each performance characteristics

Run no	MRR	F	Ra
	Larger-the-better	Smaller-the-better	Smaller-the-better
Ideal sequence	1.000	1.000	1.000
1	0.000	1.000	1.000
2	0.095	0.768	0.746
3	0.252	0.000	0.000
4	0.140	0.822	0.807
5	0.484	0.286	0.487
6	0.226	0.452	0.463
7	0.484	0.100	0.991
8	0.312	0.606	0.939
9	1.000	0.398	0.177

Table 5. Evaluation of  $\Delta_{oi}$  for each of the responses

Run no	MRR	F	Ra
Ideal sequence	1.000	1.000	1.000
1	1.000	0.000	0.000
2	0.905	0.232	0.254
3	0.748	1.000	1.000
4	0.860	0.178	0.193
5	0.516	0.714	0.513
6	0.774	0.548	0.537
7	0.516	0.900	0.009
8	0.688	0.394	0.061
9	0.000	0.602	0.823

Table 6 shows the calculated Grey relational coefficients (with the weights of  $\psi_{MRR} = 0.3$  ,  $\psi_F = 0.3$  and  $\psi_R = 0.3$  ) of each performance characteristic using Eq. (4).

Table 6. Grey relational coefficient and grey relational grade of each performance characteristics

Run no	MRR	F	Ra	Grey relational grade
Ideal sequence	1.000	1.000	1.000	
1	0.248	1.000	1.000	0.711
2	0.267	0.587	0.565	0.468
3	0.306	0.248	0.248	0.264
4	0.277	0.649	0.631	0.513
5	0.390	0.316	0.391	0.362
6	0.299	0.376	0.380	0.348
7	0.390	0.268	0.974	0.538
8	0.324	0.456	0.844	0.536
9	1.000	0.354	0.286	0.541

The Grey relational coefficients, given in Table 6, for each response have been accumulated by using Eq. (4) to evaluate Grey relational grade, which is the overall representative of all the features of cutting process quality. Thus, the multi-criteria optimization problem has been transformed into a single equivalent objective function optimization problem using the combination of Taguchi approach and Grey relational analyses. Higher is the value of Grey relational grade, the corresponding factor combination is said to be close to the optimal [3,10,11].

Triangular shaped membership function, shown in Figure 4(a), is used for fuzzy modeling of the input and output data. The five linguistic membership functions such as LOWEST, LOW, MEDIUM, HIGH and HIGHEST are used to represent the GRC of the input variables.



Figure 4: Constructed membership functions for (a) input parameters, (b) output parameter

GRG is represented by the nine membership functions such as LOWEST (L), VERY LOW (VL), MEDIUM LOW (ML), LOW, HIGH (H), MEDIUM HIGH (MHIGH), HIGHEST (H), MEDIUM, HIGHEST (MH) and ULTRA-HIGHEST (UH). Also, the triangular shaped membership function used for GRG as shown in Figure 4(b). The values of GFRG and GRG obtained for nine experiments are shown in Table 7. It is evident that the experiment number 1 and 9 exhibit the best multiple performance characteristics with the highest GFRG. Based on the grey-fuzzy calculations, the absolute average percentage error between the GRG and GFRG was calculated as 6.05%. Also, as shown in Figure 5 high correlation coefficient of  $R^2=0.987$  indicates the close relationship between GRG and GFRG.

Table 7. Comparison of GRG and GFRG

Experiment no	Grey relational grade (GRG)	Grey-fuzzy reasoning grade (GFRG)	Rank	Absolute Error %
1	0.711	0.699	1	1.755
2	0.468	0.444	6	5.440
3	0.264	0.286	9	7.746
4	0.513	0.460	5	11.522
5	0.362	0.325	7	11.323
6	0.348	0.319	8	9.064
7	0.538	0.525	3	2.476
8	0.536	0.525	4	2.095
9	0.541	0.525	2	3.048
			Average percentage error=6.05%	

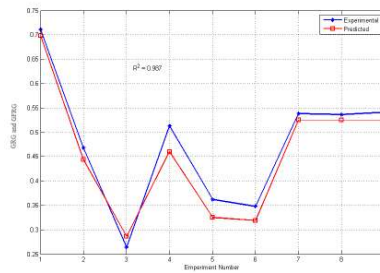


Figure 5: Comparison of experimental and fuzzy predicted GRG and GFRG

Table 8 shows the response table for the mean of GFRG. Higher is the value of GFRG, the corresponding factor combination is said to be close to the optimal [13,14]. Analysis of the means is performed for the GRFG. Based on the max-min statistics the multiple performance response is listed in Table 8. The response graph of the oblique turning parameters is plotted in Figure 8. Greater the slope of the response graph larger is the effect of the parameter on the multiple performance response [14].

Table 8. Response table for the mean Grey relational grade

Factors	Grey fuzzy relational grade			
	Level 1	Level 2	Level 3	max-min
V	0.48	0.37	0.52	0.15
f	0.56	0.43	0.38	0.18
d	0.51	0.48	0.38	0.13
Total mean Grey fuzzy relational grade= 0.46				

As indicated in Figure 6, above the mean grey fuzzy relational grade which is shown by dashed line, the optimal condition for the turning process obtained as V3f1d1.

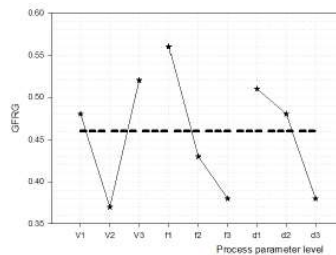


Figure 6: Response graph of GFRG for turning parameters

Analysis of variance analysis (ANOVA) is carried out to investigate which oblique turning parameters significantly affect the performance characteristic [13]. The results of ANOVA are shown in Table 9. The analysis is done at a significance level of  $\alpha = 0.05$  (confidence level of 95%). Also, the statistical testing for the experimental data was carried out using Fisher's F test for ANOVA [19]. Larger the F-value shows that the change of process parameter have more strong influence on the performance characteristic [14,25]. According to the contribution effect of the parameters, feed rate (39.13%) is found to be the major factor affecting multiple performance responses, whereas cutting speed (28.20%) and depth of cut (21.01%) are found to be the second and third ranking factor on the surface roughness, material removal rate and cutting force respectively. Also, the same contribution order is seen from the F test column of the Table 9.

Table 9. ANOVA results for GFRG

Parameter	Degree of Freedom	Sum of Square	Mean Square	F	Contribution (%)
V	2	0.039	0.019	2.39	28.20
f	2	0.054	0.027	3.34	39.13
d	2	0.029	0.015	1.82	21.01
Error	2	0.016	0.008		11.59
Total	8	0.138			100

After evaluating the optimal parameter settings, the next step is to predict and verify the enhancement of quality characteristics using the optimal parametric combination. The estimated grey-fuzzy reasoning grade  $\hat{\gamma}$  using the optimal level of the design parameters can be calculated as: given in Eq. (9) [13,14].

$$\hat{\gamma} = \gamma_m + \sum_{i=1}^o (\bar{\gamma}_i - \gamma_m) \quad (9)$$

where  $\gamma_m$  is the total mean GFRG,  $\bar{\gamma}_i$  is the GFRG at the optimal level, and  $o$  is the number of the main design parameters that affect the quality characteristics of turning process. Table 10 summarizes the results of confirmation test and optimum levels.

Table 10. Confirmation test results

Factor levels	Initial factor settings	Optimal process condition	
		Prediction	Experiment
	V1f1d1	V3f1d1	V3f1d1
MRR (mm <sup>3</sup> /min)	0.11		0.30
F (N)	123		115
Ra ( $\mu$ m)	0.87		0.65
Grey fuzzy reasoning grade (GFRG)	0.64	0.68	0.70
Improvement in grey fuzzy reasoning grade=0.06			

At the optimal setting (V3f1d1) the estimated GFRG is 0.68 and that obtained from the experiment is 0.70 which is also larger than the GFRG result of initial factor setting (0.64). Thus, a gain of 0.02 in GFRG means that the grey fuzzy logic can be successfully utilized for multi characteristics optimization problems of all the machining process [13,14].

## 5. CONCLUSIONS

This study has concentrated on the grey based fuzzy logic multi response optimization in the oblique turning process. The following conclusions can be drawn from this study.

- The grey-fuzzy algorithm is suitable for optimizing the complicated multi response machining processes,
- Output turning parameters such as surface roughness, material removal rate and cutting force are greatly improved by using grey based fuzzy logic optimization,
- ANOVA analysis showed that, table feed rate has the highest contribution (39.13%) on the multiple performance characteristics followed by the cutting speed (28.20%) and depth of cut (21.01%),
- The grey fuzzy optimization results of parameters for turning process of AISI 1050 medium carbon steel are summarized as 600 m/min cutting speed, 0.2 mm/min feed rate and 0.5 mm depth of cut.

## REFERENCES

- [1] Yang, W.H. and Tarn, Y.S. (1998). Design optimization of cutting parameters for turning operations based on the Taguchi method. *Journal of Materials Processing Technology*, vol. 84, no. 1, pp. 122-129. 10.1016/S0924-0136(98)00079-X
- [2] Esme, U. and Serin, H. (2007). A Study for the Optimization of Cutting Forces Based on the Taguchi Method. *Çukurova Üniversitesi Mühendislik Mimarlık Fakültesi Dergisi*, vol. 22, no. 1, pp. 1-12.
- [3] Kazancoglu, Y., Esme, U., Bayramoglu, M., Guven, O., and Ozgun, S. (2011). Multi-Objective Optimization of the Cutting Forces In Turning Operations Using the Grey-Based Taguchi Method *Materiali in Tehnologije*, vol. 45, no. 2, pp. 105-110.
- [4] Oxley, P.L.B. (1988). Modelling machining processes with a view to their optimization and to the adaptive control of metal cutting machine tools. *Robotics and Computer-Integrated Manufacturing*, vol. 4, no. 1, pp. 103-119. 10.1016/0736-5845(88)90065-8
- [5] Chrysosouris, G. and Guillot, M. (1990). A Comparison of Statistical and AI Approaches to the Selection of Process Parameters in Intelligent Machining. *Journal of Engineering for Industry*, vol. 112, no. 2, pp. 122-131. 10.1115/1.2899554
- [6] Yao, Y. and Fang, X.D. (1992). Modelling of multivariate time series for tool wear estimation in finish-turning. *International Journal of Machine Tools and Manufacture*, vol. 32, no. 4, pp. 495-508. 10.1016/0890-6955(92)90041-E
- [7] Zhou, C. and Wysk, R.A. (1992). An integrated system for selecting optimum cutting speeds and tool replacement times. *International Journal of Machine Tools and Manufacture*, vol. 32, no. 5, pp. 695-707. 10.1016/0890-6955(92)90024-B
- [8] Chua, M.S., Rahman, M., Wong, Y.S., and Loh, H.T. (1993). Determination of optimal cutting conditions using design of experiments and optimization techniques. *International Journal of Machine Tools and Manufacture*, vol. 33, no. 2, pp. 297-305. 10.1016/0890-6955(93)90081-5
- [9] Disney, J. and Bendell, T. (1988). The Taguchi Approach to Designing for Reliability. in *10th Advances in Reliability Technology Symposium*, G. P. Libberton, Ed. Dordrecht: Springer Netherlands, pp. 328-334.

- [10] Montgomery, D.C. (2008). Design and analysis of experiments. John Wiley & Sons.
- [11] Datta, S., Bandyopadhyay, A., and Pal, P.K. (2008). Grey-based taguchi method for optimization of bead geometry in submerged arc bead-on-plate welding. *The International Journal of Advanced Manufacturing Technology*, vol. 39, no. 11, pp. 1136-1143. 10.1007/s00170-007-1283-6
- [12] Esme, U., Bayramoglu, M., Kazancoglu, Y., and Ozgun, S. (2009). Optimization of weld bead geometry in TIG welding process using grey relation analysis and Taguchi method. *Materiali in tehnologije*, vol. 43, no. 3, pp. 143-149.
- [13] Esme, U., Kulekci, M.K., Ustun, D., Kahraman, F., and Kazancoglu, Y. (2015). Grey-based fuzzy algorithm for the optimization of the ball burnishing process. *Materials Testing*, vol. 57, no. 8, pp. 666-673. 10.3139/120.110763
- [14] Pandey, R.K. and Panda, S.S. (2014). Optimization of bone drilling parameters using grey-based fuzzy algorithm. *Measurement*, vol. 47, pp. 386-392. 10.1016/j.measurement.2013.09.007
- [15] Lin, C.L. (2004). Use of the Taguchi Method and Grey Relational Analysis to Optimize Turning Operations with Multiple Performance Characteristics. *Materials and Manufacturing Processes*, vol. 19, no. 2, pp. 209-220. 10.1081/AMP-120029852
- [16] Yang, Y.-S. and Huang, W. (2012). A grey-fuzzy Taguchi approach for optimizing multi-objective properties of zirconium-containing diamond-like carbon coatings. *Expert Systems with Applications*, vol. 39, no. 1, pp. 743-750. 10.1016/j.eswa.2011.07.067
- [17] Esme, U. (2010). Use of grey based Taguchi method in ball burnishing process for the optimization of surface roughness and microhardness of AA 7075 aluminum alloy. *Materiali in tehnologije*, vol. 44, no. 3, pp. 129-135.
- [18] Hsiao, Y.F., Tarnag, Y.S., and Huang, W.J. (2007). Optimization of Plasma Arc Welding Parameters by Using the Taguchi Method with the Grey Relational Analysis. *Materials and Manufacturing Processes*, vol. 23, no. 1, pp. 51-58. 10.1080/10426910701524527
- [19] Lim, S.-H., Lee, C.-M., and Chung, W.J. (2006). A study on the optimal cutting condition of a high speed feeding type laser cutting machine by using Taguchi method. *International journal of precision engineering and manufacturing*, vol. 7, no. 1, pp. 18-23.
- [20] Kulekci, M.K., Esme, U., Ocalir, S., Ustun, D., and Kazancoglu, Y. (2016). Tensile shear strength and elongation of FSW parts predicted by Taguchi-based fuzzy logic. *Materials Testing*, vol. 58, no. 4, pp. 351-356. 10.3139/120.110856
- [21] Zadeh, L.A. (1965). Fuzzy sets. *Information and Control*, vol. 8, no. 3, pp. 338-353. 10.1016/S0019-9958(65)90241-X
- [22] Pattnaik, S., Karunakar, D.B., and Jha, P.K. (2013). Multi-characteristic optimization of wax patterns in the investment casting process using grey-fuzzy logic. *The International Journal of Advanced Manufacturing Technology*, journal article vol. 67, no. 5, pp. 1577-1587. 10.1007/s00170-012-4591-4
- [23] Li, F.L., Xia, W., Zhou, Z.Y., Zhao, J., and Tang, Z.Q. (2012). Analytical prediction and experimental verification of surface roughness during the burnishing process. *International Journal of Machine Tools and Manufacture*, vol. 62, pp. 67-75. 10.1016/j.ijmachtools.2012.06.001
- [24] Sagbas, A. (2011). Analysis and optimization of surface roughness in the ball burnishing process using response surface methodology and desirability function. *Advances in Engineering Software*, vol. 42, no. 11, pp. 992-998. 10.1016/j.advengsoft.2011.05.021
- [25] Liu, N.-M., Horng, J.-T., and Chiang, K.-T. (2009). The method of grey-fuzzy logic for optimizing multi-response problems during the manufacturing process: a case study of the light guide plate printing process. *The International Journal of Advanced Manufacturing Technology*, journal article vol. 41, no. 1, pp. 200-210. 10.1007/s00170-008-1448-y
- [26] Ahilan, C., Kumanan, S., and Sivakumaran, N. (2009). Multi-objective optimisation of CNC turning process using grey based fuzzy logic. *International Journal of Machining and Machinability of Materials*, vol. 5, no. 4, pp. 434-451. 10.1504/ijmmm.2009.026902
- [27] Krishnamoorthy, A., Rajendra Boopathy, S., Palanikumar, K., and Paulo Davim, J. (2012). Application of grey fuzzy logic for the optimization of drilling parameters for CFRP composites with multiple performance characteristics. *Measurement*, vol. 45, no. 5, pp. 1286-1296. 10.1016/j.measurement.2012.01.008
- [28] Chiang, K.-T. and Chang, F.-P. (2006). Application of grey-fuzzy logic on the optimal process design of an injection-molded part with a thin shell feature. *International Communications in Heat and Mass Transfer*, vol. 33, no. 1, pp. 94-101. 10.1016/j.icheatmasstransfer.2005.08.006
- [29] Jean, M.-D., Lin, B.-T., and Chou, J.-H. (2006). Design of a fuzzy logic approach for optimization reinforced zirconia depositions using plasma sprayings. *Surface and Coatings Technology*, vol. 201, no. 6, pp. 3129-3138. 10.1016/j.surfcoat.2006.06.056

# Fuel properties, performance and emission characterization of waste cooking oil (WCO) in a variable compression ratio (VCR) diesel engine<sup>§</sup>

Şafak Yıldızhan<sup>1\*</sup>, Erinç Uludamar<sup>2</sup>, Ahmet Çalık<sup>3</sup>, Gonca Dede<sup>4</sup>,  
Mustafa Özcanlı<sup>5</sup>

<sup>1,5</sup>Department of Automotive Engineering, Çukurova University, Turkey

<sup>2,3</sup>Department of Automotive Engineering, Adana Science and Technology University, Turkey

<sup>4</sup>Department of Automotive Engineering, Amasya University, Turkey

## Abstract

The current study investigates the fuel properties, performance and emission characteristics in a variable compression ratio (VCR) diesel of the biodiesel produced from the waste cooking oil (WCO). The WCO samples were collected from the university and converted to biodiesel fuel with a two-step transesterification reaction. The fuel property tests showed that the properties of the WCO biodiesel were within the biodiesel standards. Diesel, WCO biodiesel and diesel-WCO biodiesel blend (B20) was used as fuel in a VCR engine. The performance and emission characteristics of the engine were measured at two different compression ratios (14:1 and 16:1) under partial load conditions. The experimental results showed that WCO biodiesel slightly decreased the brake thermal efficiency and thus increased specific fuel consumption. Biodiesel usage improved CO emissions up to 21,75% compared to diesel fuel. But, biodiesel usage increased CO<sub>2</sub> and NO<sub>x</sub> emission due to higher combustion temperature and extra oxygen content of the biodiesel.

**Keywords:** Compression ratio, Alcohol, Biodiesel, Performance, Emission

## 1. INTRODUCTION

Fossil fuels which are the main energy source for transportation of people and goods are depleting as it is known widely and the price of the fuel is increasing due to demand and supply facts [1]. Also, environmental effects of the fossil fuels threaten the human health and nature of all world. The exhaust emissions of the internal combustion engines are formed by the combustion fuels and these gases include toxic pollutants such as carbon monoxide (CO), carbon dioxide (CO<sub>2</sub>), oxides of nitrogen (NO<sub>x</sub>), unburned hydrocarbons (UHC), sulphur dioxide (SO<sub>2</sub>), and etc. These toxic gases are dangerously harmful for human health and the nature [2].

The known facts force researchers to look for alternative energy sources for internal combustion engines. Biodiesel, which can be derived from vegetable oils and animal fats has a potential of being a substitute since biodiesel fuels are less toxic and renewable [3]. Many raw materials have been studied by many researchers [1, 4-11]. Also, biodiesels are not significantly worse than fossil fuels in the means of engine performance. Biodiesels are mostly derived with transesterification reaction or thermal cracking methods. The main raw material of biodiesel are mostly non-edible vegetable oils, animal fats and waste oils. The necessity of large agricultural areas and the high effort for production of vegetable oils are one of the most important drawbacks of biodiesel usage. But, tonnes of oils are used all over the world for different purposes. Especially, the food industry produce a high amount of waste frying oil. The waste of food industries and even the waste oils used in the houses are hazardous for environment unless the wastes are managed properly. The trend of renewable processes have been started to spread recently. Even the local city corporations are aware of the huge amount of oil wastes and have some efforts on this particular subject. Recycle of waste materials is a popular research subject. Reproduction processes from the waste material are eco-friendly and economically useful since the raw materials are already used up and the unit reproduction cost can be pulled down of the original production cost in some cases.

In literature, there are many investigations on the production, performance, emission and combustion characteristics of biodiesels [12-19]. Hwang et al., (2016) published an article that investigates effects of biodiesel usage produced from

\*Corresponding author

Email: yildizhans@cu.edu.tr (Ş. Yıldızhan)

<sup>§</sup> This paper was presented in the IMSEC-2016

waste cooking oil on a compression ignition engine. The authors reported that waste cooking oil (WCO) biodiesel usage decreased the CO, hydrocarbon (HC) and smoke emissions, and also WCO biodiesel caused a slight decrement of in-cylinder pressure [20]. Man et al., (2016) reported a study that studies the effects of WCO-diesel blends on emission characteristics of a diesel engines. The study revealed that, WCO-diesel blend usage caused to increase of NO<sub>x</sub> emissions. But, CO, HC and particulate matter emission were decreased by WCO-diesel blends usage [21]. Piker et al., (2016) studied the on the biodiesel production from the waste oil bu using egg shells as catalyst. The authors reported that fatty acid methyl ester yield of 97 wt.% was obtained after 11 h at ambient temperature and pressure with egg shells [22]. In this study, fuel properties of waste cooking oil biodiesel and the effects of the biodiesel produced from waste frying oil that collected from the university on the performance and emission characteristics of a variable compression ratio (VCR) diesel engine were investigated.

## 2. METHODOLOGY

### 2.1 Experimental Fuels

The experimental study was conducted in Petroleum Research and Automotive Engineering Laboratories of the Department of Automotive Engineering at Çukurova University. Waste cooking oil (WCO) samples were used as raw material for biodiesel production. WCO biodiesel was produced with two-step transesterification reaction. First, the collected oil samples were filtered prior to reaction in order to clean the contaminants. The free fatty acid (FFA) value of the cleaned oil was measured with the standard titration method. The FFA of the WCO was measured as 1,93 wt. %. Transesterification reaction was performed twice the FFA of WCO is high. The first reaction was performed at 65°C for 60 minutes by stirring. Methanol 20 wt. % and 0,5 wt. % sodium hydroxide was used as reactant and catalyst, respectively. The methoxide was obtained before transesterification reaction by mixing methanol and sodium hydroxide. The second transesterification reaction was performed with methanol 10 wt. % and 0,25 wt. % sodium hydroxide under same conditions. After the reaction period, the mixture were batched in a separating funnel for 8 hours and at the end of the batching period the glycerine was separated from the mixture. After the separating the glycerine from the mixture, crude WCO biodiesel samples were obtained. Then, the crude biodiesel was washed with warm water and dried at 105 °C for one hour. Finally, in order to purify and to refine biodiesel the crude biodiesel was filtered. The biodiesel production flow diagram was shown in Figure 1.

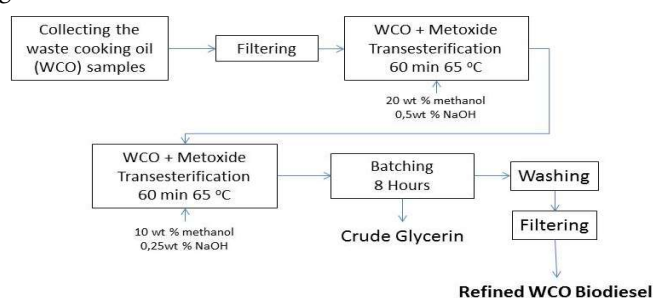


Figure 1: Biodiesel production flow diagram

In the study, low sulphur diesel fuel (conventional diesel), WCO biodiesel (waste cooking oil methyl ester), diesel-biodiesel blend B20 (80% diesel + 20% WCO) were used as fuel in a variable compression ratio (VCR) diesel engine in order to investigate the effects of waste cooking oil biodiesel on the performance and emission characteristics of a VCR diesel engine at different compression ratios.

The psychical properties of the test fuels were measured before testing them in the test engine. Instruments used for analysing the products were; Zeltex ZX 440 NIR petroleum analyser with an accuracy of  $\pm 0.5$  for determining cetane number; Tanaka AFP-102 for cold filter plugging point; Tanaka AKV-202 Auto Kinematic Viscosity test for determining the viscosity; Kyoto electronics DA-130 for density measurement, Tanaka flash point control unit FC-7 for flash point determination and IKA Werke C2000 bomb calorimeter for determination of heating value. The fuel quality measurements were performed according to EN 14214 and EN 590.

### 2.2 Experimental Setup

The performance and emission measurements were performed with a single cylinder, multi fuel, and variable compression ratio diesel engine. In order to provide the accuracy of measurements, the experiments were done at partial load conditions (60% load). An eddy current dynamometer was used to measure performance characteristics of the engine. Brake thermal efficiency (BTHE), specific fuel consumption (SFC) and exhaust gas temperature (EGT) results of the engine for test fuels were studied at two different compression ratios (14:1 and 16:1). Also, the exhaust emissions of

the engine were measured simultaneously. Carbon monoxide (CO), carbon dioxide (CO<sub>2</sub>), and nitrogen oxides (NO<sub>x</sub>) emissions were studied for all test fuels. Table 1 and 2 shows the technical specifications of the VCR test engine and exhaust gas analyser.

**Table 1** Technical specifications of the test engine

Brand	Kirloskar Oil Engines
Model	240
Configuration	Single Cylinder
Type	Four Stroke, Water Cooled
Displacement	661 cc
Bore	87.5 mm
Stroke	110 mm
Maximum/Minimum Operating Speed	2000/1200 rpm
Power	3.5 Kw @ 1500 rpm
CR range	12:1-18:1
Injection Variation	0-25 Deg BTDC
Peak Pressure	77.5 kg/cm <sup>2</sup>
Air cleaner	Paper element type
Weight	160 kg
Combustion Principle	Compression Ignition
Lubricating System	Forced Feed System

**Table 2** Technical specifications of the emission device

Brand	MRU Air Delta 1600 V
CO	0-10%
CO <sub>2</sub>	0-20%
HC	0-20000 ppm
O <sub>2</sub>	0-22%
NO	0-4000 ppm
NO <sub>2</sub>	0-1000 ppm
Lambda	0-9.99
Accuracy	According to OIML-class 1
Ambient Temperature	+5o - +45 oC
Exhaust Gas Temperature	Max 650 oC

### 3. RESULTS AND DISCUSSIONS

#### 3.1 Fuel Properties

Some important physical fuel properties test fuels were measured. The fuel properties of the diesel, WCO and B20 fuel were given in table 3. Fuel property tests shows that density of WCO and B20 was higher than the diesel fuel, but the values were within the biodiesel standards EN 14214. The tests showed that WCO biodiesel has a higher kinematic viscosity than diesel fuel. High viscosity can damage fuel pump but, the viscosity of WCO biodiesel and B20 were within the standards and it can be used directly without any modification. Heating value of the WCO biodiesel and B20 was slightly lower than diesel fuel. Flash point of the WCO biodiesel was over 120 °C which is safer compared to diesel fuel. Also, blending WCO biodiesel with diesel fuel increased the flash point value of the diesel fuel which is an important criteria for storage of the fuel. Cold filter plugging point of the WCO was measured higher than diesel fuel.

**Table 4** Fuel properties of test fuels

Fuel Properties	Test Fuels				
	Diesel	EN590	WCO Biodiesel	B20	EN 14214
Density (20 °C) kg/m <sup>3</sup>	837	820-845	889	847	860-900
Cetane Number	59,47	Min 51	51,62	53	Min 51
CFPP °C	-11	-	-5	-10	Summer<4 Winter<1
Heating Value, MJ/kg	45,856	-	39,48	44,32	-
Kinematic Viscosity (40 °C) mm <sup>2</sup> /s	2,76	2,0-4,5	4,75	3,18	3.5-5.0
Flash Point °C	79.5	Min 55	>120	93	Min 120

### 3.2 Performance Characteristics

Brake thermal efficiency (BTHE) can be defined as the ratio of power output to heat input. BTHE values are also related with heating value of the fuels. Higher BTHE value indicates the better combustion of fuel which means higher cylinder pressure and higher power output for unit fuel used. Specific fuel consumption (SFC) is a measure of how efficiently fuel is used and this value is directly related with BTHE [23]. Figure 2 and 3 shows the BTHE and SFC results of test fuels. It can be seen from the graphs increasing CR from 14:1 to 16:1 increased BTHE and decreased SFC values for all test fuels due to better combustion of fuels. Increasing CR from 14:1 16:1 increased BTHE values 2,29%, 6,75%, and 2,37% for diesel fuel, WCO biodiesel and B20 fuel, respectively. Higher compression ratio experiments resulted in 7,06%, 10,13%, and 9,92% lower SFC for diesel fuel, WCO biodiesel, and B20 fuel respectively. WCO biodiesel usage slightly decreased BTHE values compared to diesel fuel. BTHE results of WCO biodiesel were 8,62% and 4,64% lower compared to diesel fuel , at 14:1 and 16:1 compression ratios, respectively. Exhaust gas temperature (EGT) is an important criteria for internal combustion engines and it is related with combustion parameters such as compression ratio and fuel properties [24]. EGT results are shown in Figure 4. It can be seen from the graph WCO usage increased EGT compared to diesel fuel due to higher oxygen content of biodiesel. Also, increasing compression ratio increased EGT significantly for all test fuels.

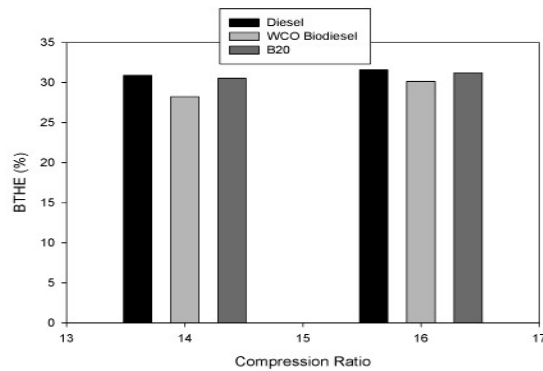


Figure 2: Brake thermal efficiency results

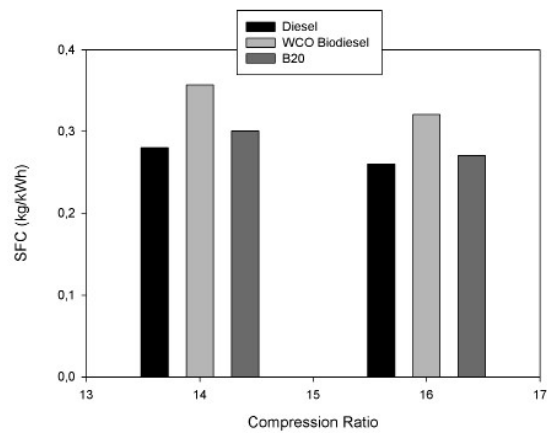


Figure 3: Specific fuel consumption results

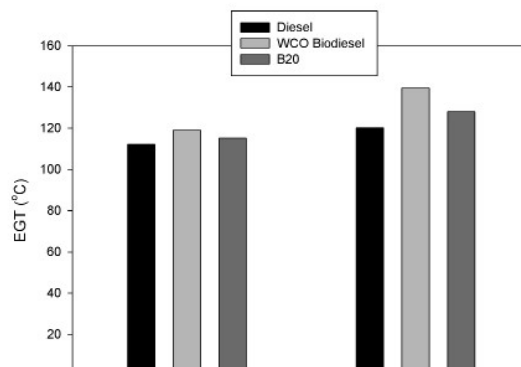


Figure 4: Exhaust gas temperature results

### 3.3 Emission Characteristics

Throughout the study; CO, CO<sub>2</sub> and NO<sub>x</sub> emissions of the test engine were measured. Figure 5, 6 and 7 shows the CO, CO<sub>2</sub> and NO<sub>x</sub> results of all test fuels, respectively. The study showed that increasing CR improved CO emissions for all test fuels due to better combustion of fuels [25]. But, CO<sub>2</sub> and NO<sub>x</sub> emissions were increased when compression ratio was elevated. Higher compression ratios enhance the combustion and thus nitrogen oxides emissions significantly elevates due to higher in-cylinder temperature and higher flame velocity. Biodiesel usage usually improves CO emissions and increases CO<sub>2</sub> and NO<sub>x</sub> emissions due to higher combustion temperature and extra oxygen content in the chemical composition [26].

Increasing CR from 14:1 to 16:1 improved CO values 34,42%, 42,03% and 34,63% for diesel fuel, WCO biodiesel and B20 fuel, respectively. But, increasing compression ratio increased CO<sub>2</sub> values 9,41%, 15,18%, and 9,40% for diesel fuel, WCO biodiesel and B20 fuel, respectively. Also, 16:1 compression ratio experiments resulted in 4,83%, 12,5%, and 9,19% higher NO<sub>x</sub> for diesel fuel, WCO biodiesel, and B20 fuel, respectively. Biodiesel usage improved CO emissions 11,47% and 21,75% for 14:1 and 16:1 compression ratios, respectively, compared to diesel fuel. But in contrary, biodiesel usage increased CO<sub>2</sub> and NO<sub>x</sub> emissions compared to diesel fuel for both compression ratios. WCO biodiesel increased CO<sub>2</sub> emissions 10,56%, and 16,39% compared to diesel fuel for 14:1 and 16:1 compression ratios, respectively. Also, WCO biodiesel increased NO<sub>x</sub> emissions 40%, and 50,23% compared to diesel fuel for 14:1 and 16:1 compression ratios, respectively.

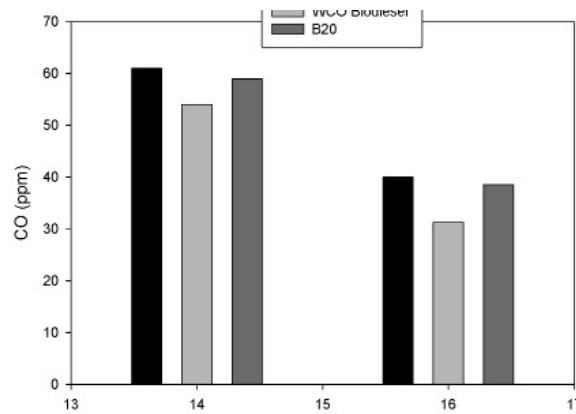


Figure 5: CO emission results

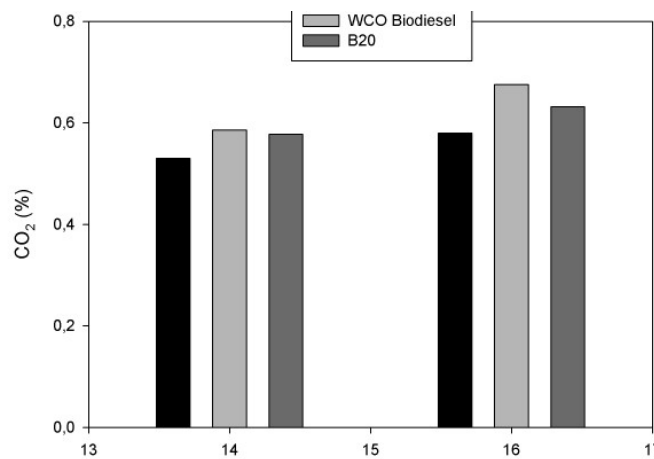


Figure 6: CO2 emission results

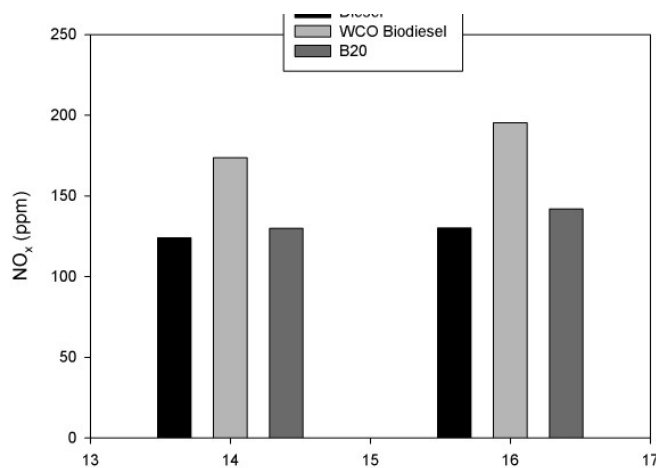


Figure 7: NO<sub>x</sub> emission results

#### 4. CONCLUSIONS

In this study waste cooking oil was converted to biodiesel by using transesterification reaction and the effects of diesel, waste cooking biodiesel and diesel-biodiesel blend usages were investigated at two different compression ratios in a variable compression ratio diesel engine. Throughout the study following conclusions were obtained;

- Waste cooking oil has a high FFA value and thus two-step transesterification was performed.
- Fuel properties of waste cooking oil and its blend with diesel fuel were within the biodiesel standards.
- Increasing compression ratio improved BTHE and SFC values, and increased EGT for all test fuels.
- Increasing compression ratio improved CO emissions but caused to increase of CO<sub>2</sub> emissions and NO<sub>x</sub> emissions.
- Waste cooking oil biodiesel usage slightly decreased BTHE and SFC values and increased EGT.
- Waste cooking oil usage improved CO emissions and caused to increase of CO<sub>2</sub> emissions and NO<sub>x</sub> emissions.

#### 5 ACKNOWLEDGEMENTS

The authors would like to thank the Cukurova University Scientific Research Project Coordination (*FBA-2016-5509*) for financial support to this project.

#### REFERENCES

- [1] Tüccar, G., Tosun, E., Özgür, T., and Aydın, K. (2014). Diesel engine emissions and performance from blends of citrus sinensis biodiesel and diesel fuel. *Fuel*, vol. 132, pp. 7-11. 10.1016/j.fuel.2014.04.065
- [2] Sajjadi, B., Raman, A.A.A., and Arandiyani, H. (2016). A comprehensive review on properties of edible and non-edible vegetable oil-based biodiesel: Composition, specifications and prediction models. *Renewable and Sustainable Energy Reviews*, vol. 63, pp. 62-92. 10.1016/j.rser.2016.05.035
- [3] Ramkumar, S. and Kirubakaran, V. (2016). Biodiesel from vegetable oil as alternate fuel for C.I engine and feasibility study of thermal cracking: A critical review. *Energy Conversion and Management*, vol. 118, pp. 155-169. 10.1016/j.enconman.2016.03.071
- [4] Akar, M.A. (2016). Performance and emission characteristics of compression ignition engine operating with false flax biodiesel and butanol blends. *Advances in Mechanical Engineering*, vol. 8, no. 2, pp. 1-7. 10.1177/1687814016632677
- [5] Farooq, M., Ramli, A., and Naem, A. (2015). Biodiesel production from low FFA waste cooking oil using heterogeneous catalyst derived from chicken bones. *Renewable Energy*, vol. 76, pp. 362-368. 10.1016/j.renene.2014.11.042
- [6] Iglesias, L., Laca, A., Herrero, M., and Díaz, M. (2012). A life cycle assessment comparison between centralized and decentralized biodiesel production from raw sunflower oil and waste cooking oils. *Journal of Cleaner Production*, vol. 37, pp. 162-171. 10.1016/j.jclepro.2012.07.002
- [7] Issariyakul, T. and Dalai, A.K. (2010). Biodiesel Production from Greenseed Canola Oil. *Energy & Fuels*, vol. 24, no. 9, pp. 4652-4658. 10.1021/ef901202b
- [8] Predojevic, Z., Skrbic, B., and Djuricic-Mladenovic, N. (2012). Transesterification of linoleic and oleic sunflower oils to biodiesel using CaO as a solid base catalyst. *Journal of the Serbian Chemical Society*, vol. 77, no. 6, pp. 815-832. <https://doi.org/10.2298/JSC110824206P>

- [9] Sootchiewcharn, N., Attanatho, L., and Reubroycharoen, P. (2015). Biodiesel Production from Refined Palm Oil using Supercritical Ethyl Acetate in A Microreactor. *Energy Procedia*, vol. 79, pp. 697-703. 10.1016/j.egypro.2015.11.560
- [10] Wittoon, T., Bumrungsalee, S., Vathavanichkul, P., Palitsakun, S., Saisriyoot, M., and Faungnawakij, K. (2014). Biodiesel production from transesterification of palm oil with methanol over CaO supported on bimodal meso-macroporous silica catalyst. *Bioresource Technology*, vol. 156, pp. 329-334. 10.1016/j.biortech.2014.01.076
- [11] Yücel, Y. (2011). Biodiesel production from pomace oil by using lipase immobilized onto olive pomace. *Bioresource Technology*, vol. 102, no. 4, pp. 3977-3980. 10.1016/j.biortech.2010.12.001
- [12] Ozcanli, M., Akar, M.A., Calik, A., and Serin, H. (2017). Using HHO (Hydroxy) and hydrogen enriched castor oil biodiesel in compression ignition engine. *International Journal of Hydrogen Energy*. 10.1016/j.ijhydene.2017.01.091
- [13] Serin, H., Yildizhan, S., Akar, M.A., and Ozcanli, M. (2016). Methodological effects of thermal cracking and transesterification on fuel specifications of false flax biodiesel. *Journal of Biotechnology*, vol. 231, p. S47. 10.1016/j.jbiotec.2016.05.179
- [14] Serin, H. and Akar, N.Y. (2013). The Performance and Emissions of a Diesel Engine Fueled with Tea Seed (*Camellia sinensis*) Oil Biodiesel-Diesel Fuel Blends. *International Journal of Green Energy*, vol. 11, no. 3, pp. 292-301. 10.1080/15435075.2013.773434
- [15] Serin, H., Ozgur, C., Ozcanli, M., Aydin, K., and Ozgur, T. (2013). Preparation of fuels by cracking of different plastics and their blends with diesel fuel. *Current Opinion in Biotechnology*, vol. 24, p. S44. 10.1016/j.copbio.2013.05.097
- [16] Tosun, E., Ozgur, T., Ozgur C., Ozcanli, M., Serin, H., Aydin, K. (2017). Comparative analysis of various modelling techniques for emission prediction of diesel engine fueled by diesel fuel with nanoparticle additives. *European Mechanical Science* vol. 1, no. 1, pp. 15-23.
- [17] Özcanli, M., Serin, H., Saribiyik, O.Y., Aydin, K., and Serin, S. (2012). Performance and Emission Studies of Castor Bean (*Ricinus Communis*) Oil Biodiesel and Its Blends with Diesel Fuel. *Energy Sources, Part A: Recovery, Utilization, and Environmental Effects*, vol. 34, no. 19, pp. 1808-1814. 10.1080/15567036.2010.545800
- [18] Çelebi, K., Uludamar, E., and Özcanlı, M. (2017). Evaluation of fuel consumption and vibration characteristic of a compression ignition engine fuelled with high viscosity biodiesel and hydrogen addition. *International Journal of Hydrogen Energy*, <https://doi.org/10.1016/j.ijhydene.2017.02.066>
- [19] Saribiyik, O.Y., Özcanlı, M., Serin, H., Serin, S., and Aydın, K. (2011). Biodiesel Production from *Ricinus Communis* Oil and its Blends with Soybean Biodiesel. *Strojniški vestnik – Journal of Mechanical Engineering*, 10.5545/sv-jme.2009.054
- [20] Hwang, J., Bae, C., and Gupta, T. (2016). Application of waste cooking oil (WCO) biodiesel in a compression ignition engine. *Fuel*, vol. 176, pp. 20-31. 10.1016/j.fuel.2016.02.058
- [21] Man, X.J., Cheung, C.S., Ning, Z., Wei, L., and Huang, Z.H. (2016). Influence of engine load and speed on regulated and unregulated emissions of a diesel engine fueled with diesel fuel blended with waste cooking oil biodiesel. *Fuel*, vol. 180, pp. 41-49. 10.1016/j.fuel.2016.04.007
- [22] Piker, A., Tabah, B., Perkasi, N., and Gedanken, A. (2016). A green and low-cost room temperature biodiesel production method from waste oil using egg shells as catalyst. *Fuel*, vol. 182, pp. 34-41. 10.1016/j.fuel.2016.05.078
- [23] Amarnath, H.K., Prabhakaran, P., Bhat, S.A., and Paatil, R. (2014). A Comparative Analysis of Thermal Performance And Emission Characteristics of Methyl Esters of Karanja And *Jatropha* Oils Based on A Variable Compression Ratio Diesel Engine. *International Journal of Green Energy*, vol. 11, no. 7, pp. 675-694. 10.1080/15435075.2013.777905
- [24] Mohanraj, T. and Mohan Kumar, K.M. (2013). Operating Characteristics of a Variable Compression Ratio Engine Using Esterified Tamanu Oil. *International Journal of Green Energy*, vol. 10, no. 3, pp. 285-301. 10.1080/15435075.2011.653849
- [25] Vasudeva, M., Sharma, S., Mohapatra, S.K., and Kundu, K. (2016). Performance and exhaust emission characteristics of variable compression ratio diesel engine fuelled with esters of crude rice bran oil. *SpringerPlus*, journal article vol. 5, no. 1, p. 293. 10.1186/s40064-016-1945-7
- [26] Chavan, S.B., Kumbhar, R.R., Kumar, A., and Sharma, Y.C. (2015). Study of Biodiesel Blends on Emission and Performance Characterization of a Variable Compression Ratio Engine. *Energy & Fuels*, vol. 29, no. 7, pp. 4393-4398. 10.1021/acs.energyfuels.5b00742

# District heating and power generation based flue gas waste heat recovery<sup>§</sup>

Caglar Karaoglu<sup>1</sup>, Arif Ozbek<sup>2\*</sup>

<sup>1</sup>Cukurova University, Institute of Natural and Applied Sciences, Mechanical Engineering Department, Adana, Turkey

<sup>2</sup>Cukurova University, Ceyhan Engineering Faculty, Mechanical Engineering Department, Adana, Turkey

## Abstract

In this study, integration of appropriate renewable methods are going to be applied on conventional coal fired steam power plant which has 660 MW full load capacity and including 4 Turbines (1 HP, 1 IP and 2 LP), one Benson type boiler and having multi pre heater stages for each unit. Steam parameters are 177 Bar and 541 °C super-heater section and 50 bar 539 °C for re-heater section. Primary fuel is coal except for startup and shut down operations. It is aimed by retrofitting some renewable energy methods on existing power plant, thus eliminating conventional type power plants adverse effects on thermodynamically, environmental and economic issues.

One of the most important issue of conventional steam power plant operation is waste heat recovery management. A widespread techniques has been developed on this topic. It's possible to handle low grade heat by considering thermodynamic and environmental facts and also dealing with restrictions and opportunities after fulfilled feasibility study. In this study, it is being proposed waste heat recovery by combining Organic-Rankine Cycle (ORC) with steam-Rankine cycle at available section. Brief summary of operation is ORC takes place after regenerative air preheater section and the target is to utilize waste heat of flue gas either via district heating or power generation up to few MW values. Depending upon the calculation and results additional modifications can further be needed as well.

**Keywords:** Waste heat recovery, flue gas, steam power plant

## 1. INTRODUCTION

Energy is the power and vital part of life. In the future, we must have a sustainable, affordable and environment friendly energy supply. Conventional fossil energy sources will be replaced by renewable sources, gradually. Renewable technologies are considered as clean sources of energy and optimal use of these resources minimize environmental impacts, produce minimum secondary wastes and are sustainable based on current and future economic and social needs. [1].

A major challenge for the future electric grid is to integrate renewable power sources such as solar, wind and biomass [2]. Such sources are variable and intermittent, unlike traditional sources that provide a controllable, steady stream of power. Instead of fully replacing renewable by conventional systems, it's better to implement partial integration of renewable methods on such conventional power plants already in operation.

Renewable energy systems are increasingly being used for electricity generation, either at small-scale decentralized systems with capacity in the kW scale or even medium-scale systems (often called utility-scale) with capacity of a few MW. However, the large-scale systems with capacity of some hundreds of MW are still using conventional technologies based on fossil fuels.

One of the most important disadvantages of conventional technologies is the environmental impact. The combustion of fossil fuels leads to the inevitable production of carbon dioxide (CO<sub>2</sub>), while most of the times harmful emissions are produced, such as carbon monoxide (CO), nitrogen oxides (NOX), sulfur oxides (SOX), unburned hydrocarbons (HC), and solid particles. Another critical disadvantage of conventional technologies is that they need continuous fuel supply to operate, which contributes to the operating costs.

On the other hand, renewable energy technologies do not require any fossil fuel during normal operation. Their operation is based on the exploitation of natural resources, such as the sun and wind, having relatively lower operating costs,

\*Corresponding author

Email: arozbek@cu.edu.tr (A. Özbek)

<sup>§</sup>This paper was presented in the IMSEC-2016

although they still require some maintenance. The most important disadvantage of renewable energy technologies is the fluctuation of their power output [5].

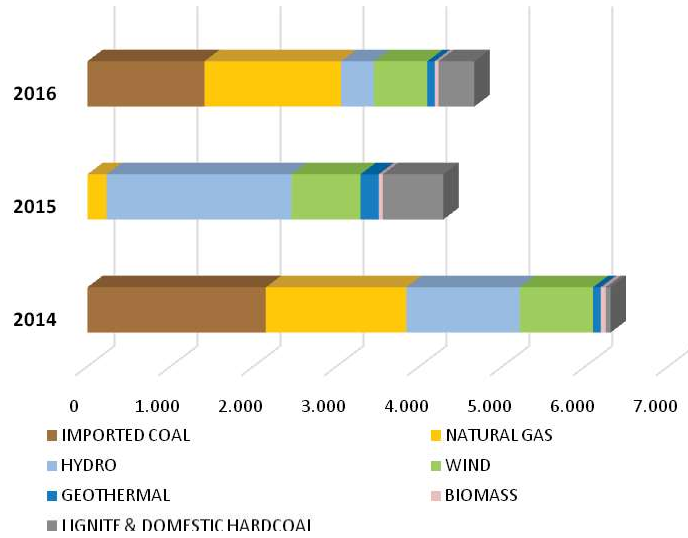


Figure 1: Additional Installed Capacity by years

It is generally expected that coal will continue to play a key role in the future energy mix as it is the most abundant and cheapest fossil fuel source. Such solid fossil fuels are combusted in steam power plants, where the power cycle is based on the steam-Rankine thermodynamic cycle, using a steam turbine.

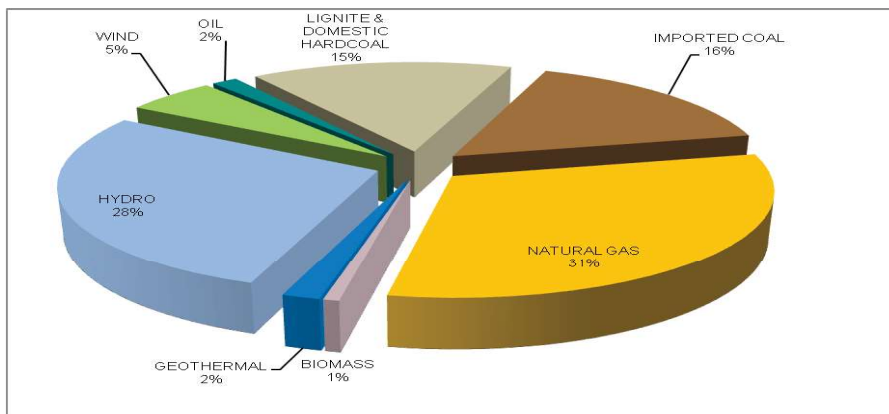


Figure 2: Electricity Generation Distribution Depend on Energy Sources (2016)

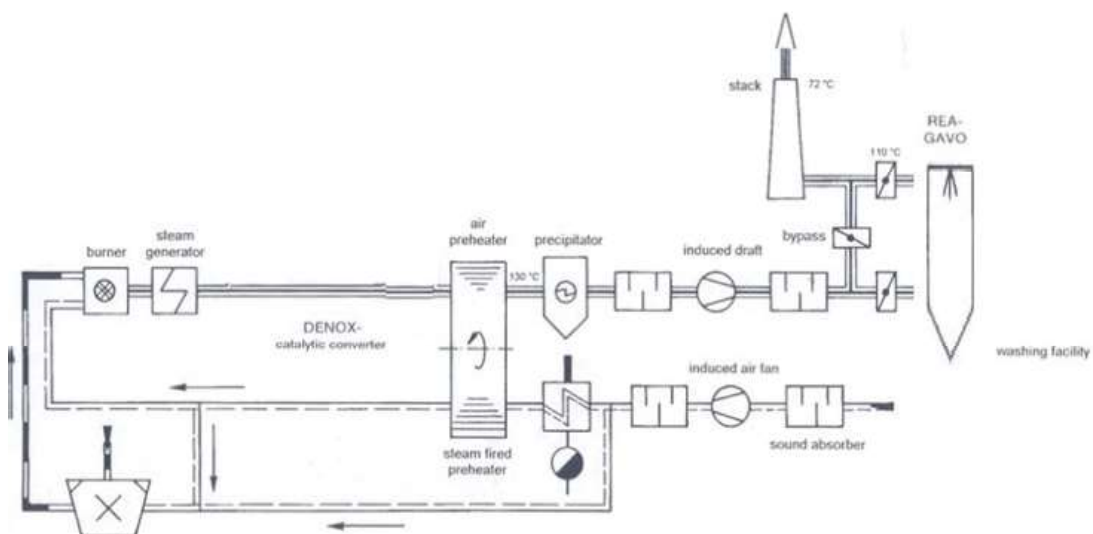


Figure 2: A path of Air/Flue-gas

Additionally, pulverized coal firing system, integrated with its components, in the steam generator (boiler) is to provide through the combustion of certain bituminous coals the necessary thermal energy for the generation of steam which in turn is required for driving the downstream turbine with downstream generator for power generation. Flue gases leaving the boiler combustion chamber pass over the convection banks of the super-heaters, re-heaters and then enter regenerative air heater. There the gases exchange their thermal energy with the primary and secondary air. The temperature of the gas entering the air heater is reduced from about 400 °C to 150 °C. The cooled gases then pass to electrostatic precipitator where most of the dust is removed. Via induced draft fan, the cleaned gases then pass to the FGD plant for desulfurization and then to atmosphere via the stack [4].

It is possible to see several studies that deal with renewable energy integration to conventional systems related to thermodynamic analysis.

## 1.1 Literature Survey

Gang Xu et al. (2014) studied integration of waste heat recovery system on flue gas path. To achieve extra work, installed low temperature economizer after ESP takes place. Exergy analysis and economic analysis have been done and discussed on results [6].

C. Li et al. (2016) investigated on generated waste heat quantities during industrial production. In order to maximize net power output, an optimal combination of cycle configuration, fluid and cycle parameters under different heat source condition, the following researches have been performed. To sum up, results indicate that the regenerative organic trans-critical cycle produces the maximum power output at source temperatures up to about 500 °C, and different optimum working fluids are obtained under different heat source temperature [7].

Chengyu Li et al. (2016) has been studied for waste heat recovery from flue gas in a wide range temperature. The study also dealing with optimum relationship between selected fluid and heat source in order to achieve better thermal efficiency. Evaluation, optimization comparison of many cycles has been evaluated.

Xiaoqu Han et al. (2016) studied on flue gas waste heat recovery method by extracting water from high moisture lignite coal thus yielding increase of boiler efficiency. Energy saving potential has also been evaluated. To achieve this, different options take into consideration like economizer or spray tower. Thermodynamic and economic performance of system are investigated for each scheme [8].

Jiayi Xia et al. (2016) performed thermo - economical analysis of combined system which is named combined cooling and power system for engine waste heat recovery. Vital part of the system thermodynamically based were studied. Exer-go-economic evaluation is another branch of this study. Via the single-objective optimization, the lowest average cost per unit of exergy product for the overall system is obtained [9].

Navid Nazaria et al. (2016) proposed multi objective optimization of combined steam& ORC based on exergy and exer-go-economic analysis of waste heat recovery application. Combined cycle has been performed in terms of exer-go-economic and exergy efficiency. Total product cost rate and exergy efficiency were cornerstone of this study. Three different type fluid selection has been monitored to perform system characteristic as well [10].

Zhenying Wang et al. (2016) has been presented evaluation of flue gas waste heat and water recovery from a fossil fuel boilers. Several parameters has been studied like efficient heat and water recovery for various kinds of fossil fuel boilers, heat recovery dependency parameters like moisture content [11].

Xiling Zhao et al. (2016) presented another waste heat recovery method, known peak shaving heat pump. This study consist of improving transmission network and distribution capacity, Also study proposed by heating capacity, and reduced heating energy consumption. As such, the proposed system is advantageous in terms of energy saving, emission reduction, and economic benefits [12].

## 2. MATERIAL AND METHOD

In this study, integration of appropriate renewable methods are going to be applied on conventional coal fired steam power plant which has 660 MW full load capacity and including 4 Turbines (1 HP,1 IP and 2 LP), one Benson type boiler and having multi pre heater stages for each unit. Steam parameters are 177 bar and 541 °C super-heater section and 50 bar 539 °C for re-heater section. Primary fuel is coal except for start up and shut down operations. It is aimed by retrofitting some renewable energy methods on existing power plant, thus eliminating conventional type power plants adverse effects on thermodynamically, environmental and economic issues.

One of the most important issue of conventional steam power plant operation is waste heat recovery management. A widespread techniques has been developed on this topic. It's possible to handle low grade heat by considering thermodynamic and environmental facts and also dealing with restrictions and opportunities after fulfilled feasibility study. In

this study, it is being proposed waste heat recovery by combining Organic-Rankine cycle with steam-Rankine cycle at available section. Brief summary of operation is ORC takes place after regenerative air preheater section and the target is to utilize waste heat of flue gas either via heating or power generation up to few MW values. Depending upon the calculation and results additional modifications can further be needed as well.

However, the aim of an ORC machine is the power generation and as secondary purpose cogeneration or tri generation with hot water production for heating/cooling.

As seen below figure waste heat recovery is the highest temperature recovery ORC application. The higher temperature available the higher conversion capability means the higher efficiency of cycle thus reduction of waste energy and heat.

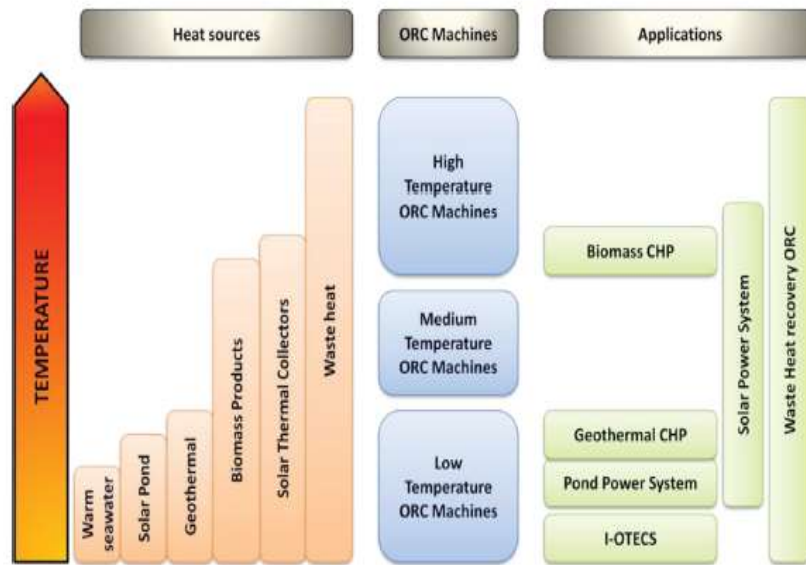


Figure 3: ORC Applications

## 2.1 District Heating & Internal Process Heating Based Flue gas Heat Recovery

The temperature of the flue gas upstream of the absorbers is around 140-150 °C and the volumetric flow is ~760m<sup>3</sup>/s. Therefore there is considerable heat potential, if it can be utilised in an appropriate and efficient way. It is assumed that the temperature at the outlet of the absorber (inlet of the stack) doesn't change or change marginally because of water / steam saturation effect. Indeed if the flue gas inlet temperature of the absorber is lower, then less heat energy is provided into the FGD system and less amount of water will be vaporized.

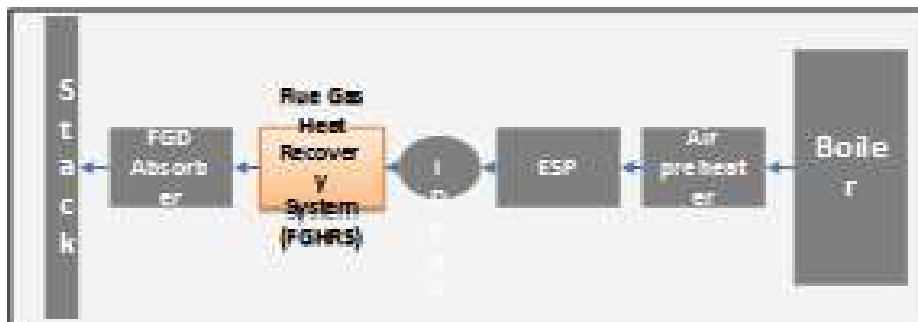


Figure 4: Flue gas heat recovery system

As it known that steam power plant have waste energy, it should be decreased to enhance efficiency so ORC will be placed out of boiler to recover energy, proper fluid selection which is used as refrigerant in ORC, is very important section while dealing with relatively lower energy conversion studies. Although there is considerable heat potential, it can only be of feasible usage if there is a continuous consumer. Evaluation both internal and external consumer options will also be considered in this study. Internal options can be accounted first feed water preheating or to heat primary air that will increase combustion efficiency in the air/flue gas system. Besides, it is possible to heat clean gas in the stack in order to prevent visible plume and it can also help to create additional vacuum in the stack which may help IDE.

## 2.2 Power Generation Based Flue gas Heat Recovery

In this chapter, it is going to be evaluated a potential of residual flue gas temperature which is around 400 °C medium temperature before air heater section. In order to utilize that great potential waste heat after combustion process, regenerative air pre-heater has been settled down to handle heat transfer between flue gas and fresh air. Normal operation conditions described as follows:

Multi flow designs like tri and quart sector shaped air heater allow preheating of primary and secondary air in one air heater. Specially with respect to the high pressure difference between primary air and flue gas double seal system minimize leakage of primary air into the flue gas.

Instead using regenerative air pre heater alternative recovery method can be implemented at available flue gas path. Power generation based ORC integration is main idea of this study that is proposed converting a great waste heat of flue gas into electric generation via ORC. A proper fluid selection, ORC equipment (ORC pump, evaporator, turbine, condenser), exergo - economic analysis, data table, graphs are main study cases. Thus depending on cycle efficiency up to a few MW can be obtained by flue gas waste heat recovery.

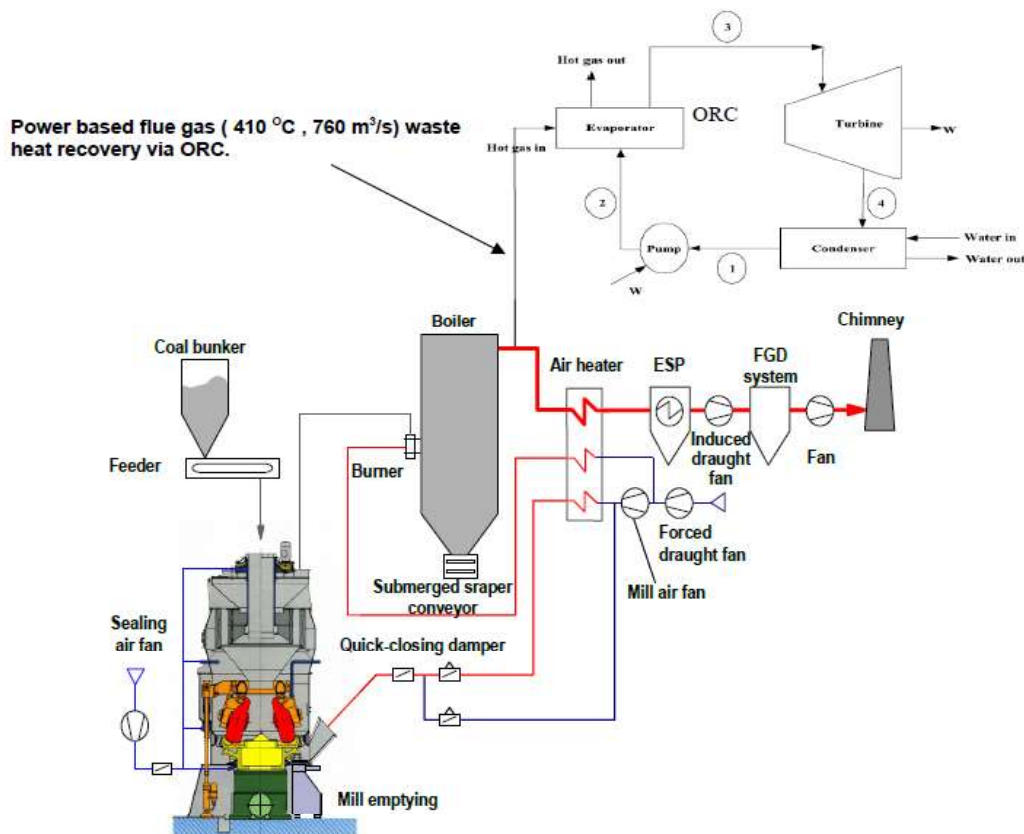


Figure 4 : Air / Flue gas system integration with power generation based flue gas waste heat recovery via ORC

## 3. RESULT AND DISCUSSION

In this chapter, it is going to be discussed the expectations on waste heat recovery benefits, expenditures and losses, heat gains and comparison between conventional type systems and renewable integrated systems. All parameters needed to calculate thermodynamic laws which are actually first law of thermodynamic and second law of thermodynamic, is taken from coal fired steam power plant. Those are mainly flow rate of flue gas, temperature of flue gas, pressure of flue gas and whatsoever needed. Basic expectations are described as follows:

Higher efficiency

Reduction wastes

Lower operating costs

Decreasing adverse environmental effect of main fuel ( coal )

The calculations and discussion topics are going to be performed are below:

Energy analysis : First Law of Thermodynamic

Exergy analysis : Second Law of Thermodynamic

Exergo economic analysis: Cost analysis of exergy loss & annual saving, investment options for necessary part.

Environmental analysis : Impacts in emission (CO<sub>2</sub> emission )

To sum up, one of the weaken part of conventional type power plant is waste heat regeneration that exist on flue gas path. By using ORC combined with Steam Rankine Cycle, total losses will be minimized via integrating waste heat recovery system on flue gas path thereby energy conversion takes more efficiently into either heating or power based theory. Depending upon the consumer opportunities, heating based project is going to be justified while decision procedure. Consumer options are seem to be external as district heating or internal options as feed water preheating, combustion air preheating or clean gas preheating.

## REFERENCE LIST

- [1] NREL. Dollars From Sense: The Economic Benefits of Renewable Energy Retrieved. November 24 2013.
- [2] United States Senate, One Hundred Eleventh Congress. First Session to Receive Testimony on a Majority Staff Draft for a Renewable Electricity Standard Proposal, Hearing before the Committee on Energy and Natural Resources; U.S. Government Printing Office; February 2009.
- [3] Froese R.E., Shonnard D.R., Miller C.A., Koers K.P. and Johnson D.M. (2010). An evaluation of greenhouse gas mitigation options for coal-fired power plants in the US Great Lakes States. *Biomass and Bioenergy* vol. 34 no. 3, p. 251-262.
- [4] Babcock Operating/Maintanance Manual System Description for training Steam Generator.
- [5] Kosmadakis G., Manolakos D., Papadakis G. (2011). Simulation and economic analysis of a CPV/thermal system coupled with an organic Rankine cycle for increased power generation. *Solar Energy*, vol. 85 no. 2, p. 308–324.
- [6] Xu G., Huang S.W. and Yang Y.P. (2013). Techno-economic analysis and optimization of the heat recovery of utility boiler flue gas; *Applied Energy*, vol. 112, p. 907-917.
- [7] Chengyu L. and Huaixin W. (2016). Power cycles for waste heat recovery from medium to high temperature. *Applied Energy*, vol. 180, p. 707–721.
- [8] Xiaoqu H., Junjie Y., Sotirios K. , Ming L., Kakaras E. and Feng X. (2016). Water extraction from high moisture lignite by means of efficient integration of waste heat and water recovery technologies with flue gas pre-drying system. *Applied Thermal Engineering*, vol.110, pp.442–456.
- [9] Jiayi X., Jiangfeng W., Juwei L., Pan Z. and Yiping D. (2016). Thermo-economic analysis and optimization of a combined cooling and power (CCP) system for engine waste heat recovery. *Energy Conversion and Management*, vol. 128, p. 303–316.
- [10] Navid N., Parisa H. and Soheil P. (2016). Multi-objective optimization of a combined steam-organic Rankine cycle based on exergy and exergo-economic analysis for waste heat recovery application. *Energy Conversion and Management*, vol. 127, p. 366–379.
- [11] Zhenying W., Xiaoyue Z., Zhen L. (2016). Evaluation of a flue gas driven open absorption system for heat and water recovery from fossil fuel boilers. *Energy Conversion and Management*, vol. 128, p. 57–65.
- [12] Xiling Z., Lin F., Xiaoyin W., Tao S., Jingyi W. and Shigang Z. (2016). Flue gas recovery system for natural gas combined heat and power plant with distributed peak-shaving heat pumps. *Applied Thermal Engineering*, vol. 111, p. 599–607.

# Thermodynamic Analysis of Bus Air Conditioner Working with Refrigerant R600a

Mehmet Bilgili<sup>1\*</sup>, Ediz Cardak<sup>2</sup>, Arif Emre Aktas<sup>3</sup>

<sup>1</sup>Cukurova University, Automotive Engineering Department, Turkey

## Abstract

Refrigerant R134a (tetrafluoroethane) is widely used in automotive air conditioners and has a good performance. However, since refrigerant R134a still has a high global warming potential (GWP), this refrigerant must be replaced with environmentally friendly refrigerants such as R600a (isobutane), which is a natural fluid, no effect on the climate, inexpensive and readily available. In this study, thermodynamic analysis of a bus air conditioner working with refrigerant R600a was performed. Adana province of Turkey was chosen as the study region. Firstly, a bus used for inter-city passenger transportation with a passenger capacity of 56 persons was selected. Cooling Load Hourly Analysis Program (HAP) was used to determine the hourly cooling load capacity of the selected inter-city bus model. Useful and reversible works of compressor, coefficient of performance (COP), exergy efficiency and exergy destructions of the bus air conditioning system were obtained and evaluated in detail.

**Keywords:** Air-conditioning, refrigerant R600a, air mixing ratio, exergy, exergy efficiency, intercity bus.

## 1. INTRODUCTION

Today, the development of industrialization and technology has brought many advantages, such as efficient production, cheaper price and thus improved quality of life. On the other hand, global energy demand has shown a significant increase due to rising technological and population growth, and at the same time, unfortunately, fossil fuels have been sharply declining. In this respect, the global warming being the threat of climatic change, efficient usage of energy sources and greenhouse-gas (GHG) emissions based on fossil energy consumption have become most attractive issues in the present decade [1].

With steady temperature increase throughout the years, the importance of air-conditioning (AC) systems is becoming more important part of our lives day by day. AC systems have great importance in transportation as well. The comfort of the passengers is as important as the energy efficiency of vehicles. An ideal automobile air-conditioning (AAC) system reduces temperature and humidity which can impact on our thermal comfort and air quality. The system also reduces dehydration level and thus excessive sweating [2]. The importance of AC becomes clearer, especially when hot temperatures being experienced. On the other hand, AAC systems and most of their components, regardless of their benefits, consume great amounts of energy.

The number of buses and total vehicles is increasing rapidly in Turkey and the world. With growing numbers of vehicles, energy efficiency becomes more important in public transportation. It is worthwhile to mention that buses are one of the most important figures of public transportation and they are designed to carry many passengers. Automotive air conditioning (AAC) systems are the second largest energy consumers in vehicles including buses [3]. To reduce fuel consumption of an inter-city bus, increasing the energy efficiency of inter-city bus AC system should take into consideration.

There are several available refrigerants for AC systems. R404a, R410a, R502, R507, R22, R290, R134a, R500 and, R600a refrigerants are some of them. Refrigerant R134a (tetrafluoroethane) is widely used in automotive air conditioners and has good performance. However, since refrigerant R134a still has a high global warming potential (GWP), this refrigerant must be replaced with environmentally friendly refrigerants such as R600a (isobutane), which is a natural fluid, no effect on the climate, inexpensive and readily available. In this study, thermodynamic analysis of bus air conditioner working with refrigerant R600a was performed. Total exergy destruction and overall exergy efficiency of system were obtained and evaluated in detail.

\*Corresponding author

Email: mbilgili@cu.edu.tr (M. Bilgili)

<sup>3</sup>This paper was presented in the IMSEC-2016

## 2. MATERIAL AND METHODS

A schematic view of the inter-city bus AC system is presented in Figure 1. As seen from the figure, the outside fresh air is firstly mixed with re-circulated air to satisfy the ventilation requirement. Then, the mixed air flows through a cooling coil (evaporator), and it is supplied to the cabin by the evaporator fan. Standard inter-city bus AC system components are compressor, evaporator, expansion valve and condenser.

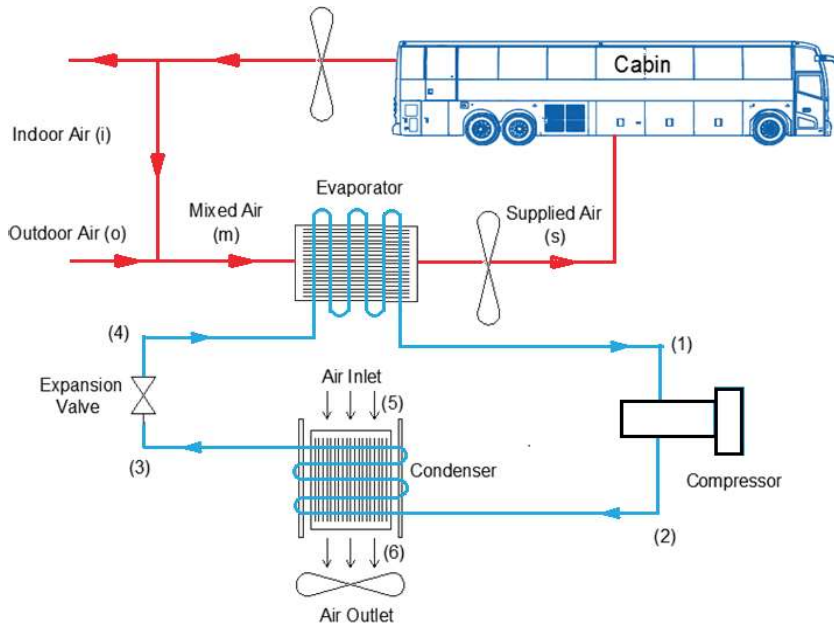


Figure 1. Schematic view of the inter-city bus AC system

The mass flow rate of outdoor air,  $\dot{m}_o$ , and the mass flow rate of indoor air,  $\dot{m}_i$ , are mixed at a constant pressure and certain rate. The value of air mixing ratio, MR is defined by:

$$MR = \frac{\dot{m}_o}{\dot{m}_i} \quad (1)$$

From the mass balance of dry air and water vapor:

$$\dot{m}_s = \dot{m}_o + \dot{m}_i = \dot{m}_m \quad (2)$$

$$\dot{m}_m \cdot w_m = \dot{m}_o \cdot w_o + \dot{m}_i \cdot w_i \quad (3)$$

From the energy balance:

$$\dot{m}_m \cdot h_m = \dot{m}_o \cdot h_o + \dot{m}_i \cdot h_i \quad (4)$$

The sensible cooling load,  $\dot{Q}_{\text{sensible,bus}}$ , and the latent cooling load,  $\dot{Q}_{\text{latent,bus}}$ , on the inter-city bus are given by:

$$\dot{Q}_{\text{sensible,bus}} = \dot{m}_s \cdot c_p \cdot (T_i - T_o) \quad (5)$$

$$\dot{Q}_{\text{latent,bus}} = \dot{m}_s \cdot h_{fg} \cdot (w_i - w_o) \quad (6)$$

By-pass factor, BPF can be calculated as:

$$BPF = \frac{T_s - T_{ADP}}{T_m - T_{ADP}} \quad (7)$$

where  $T_s$ ,  $T_{ADP}$  and  $T_m$  are the supplied air temperature, the coil apparatus dew-point temperature and the mixed air temperature, respectively. The optimum capacity of the cooling coil,  $\dot{Q}_{\text{evaporator}}$ , can be obtained from energy balance across the cooling coil [4]:

$$\dot{Q}_{\text{evaporator}} = \dot{m}_s \cdot (h_m - h_s) - \dot{m}_w \cdot h_w \quad (8)$$

where  $h_w$  and  $\dot{m}_w$  are the enthalpy of condensate leaving the cooling coil (evaporator) and mass flow rate of condensate on the cooling coil, respectively.  $\dot{m}_w$  can be calculated as follows:

$$\dot{m}_w = \dot{m}_s \cdot (w_m - w_s) \quad (9)$$

The general exergy balance is written as:

$$\dot{E}x_{\text{in}} - \dot{E}x_{\text{out}} = \dot{E}x_{\text{dest}} \quad (10)$$

where  $\dot{E}x_{\text{in}} - \dot{E}x_{\text{out}}$  is the rate of net exergy transfer by work, heat and mass. Moreover, the rate of net exergy destruction is indicated with  $\dot{E}x_{\text{dest}}$  in the equation above. The general exergy balance can also be written in the rate form as [5]:

$$\dot{E}x_{\text{heat}} - \dot{E}x_{\text{work}} + \dot{E}x_{\text{mass,in}} - \dot{E}x_{\text{mass,out}} = \dot{E}x_{\text{dest}} \quad (11)$$

Besides, the rate of formation of the general exergy balance is evaluated as:

$$\sum \left(1 - \frac{T_0}{T_k}\right) \cdot \dot{Q}_k - \dot{W} + \sum (\dot{m}_{\text{in}} \cdot ex_{\text{in}}) - \sum (\dot{m}_{\text{out}} \cdot ex_{\text{out}}) = \dot{E}x_{\text{dest}} \quad (12)$$

where  $\dot{W}$  and  $ex$  are the work rate and the flow (specific) exergy, respectively. Additionally, the properties at the reference (dead) state of  $P_0$  and  $T_0$  are shown as subscript zero. The specific flow exergy of refrigerant or air can be calculated from the following equation:

$$ex_{\text{ref,air}} = (h - h_0) - T_0 \cdot (s - s_0) \quad (13)$$

The exergy rate is calculated as:

$$\dot{E}x = \dot{m} \cdot (ex) \quad (14)$$

The exergy efficiency of various steady-flow devices,  $\psi$ , can also be expressed as:

$$\psi = \frac{\dot{E}x_{\text{out}}}{\dot{E}x_{\text{in}}} = \frac{\text{Exergy recovered}}{\text{Exergy supplied}} \quad (15)$$

$\text{COP}_{\text{ref}}$  which is an energy-based efficiency measure of the refrigeration unit is calculated from the following equation:

$$\text{COP}_{\text{ref}} = \frac{\dot{Q}_{\text{evap}}}{\dot{W}_{\text{comp}}} \quad (16)$$

The reversible power,  $\dot{W}_{\text{rev}}$ , can be defined as:

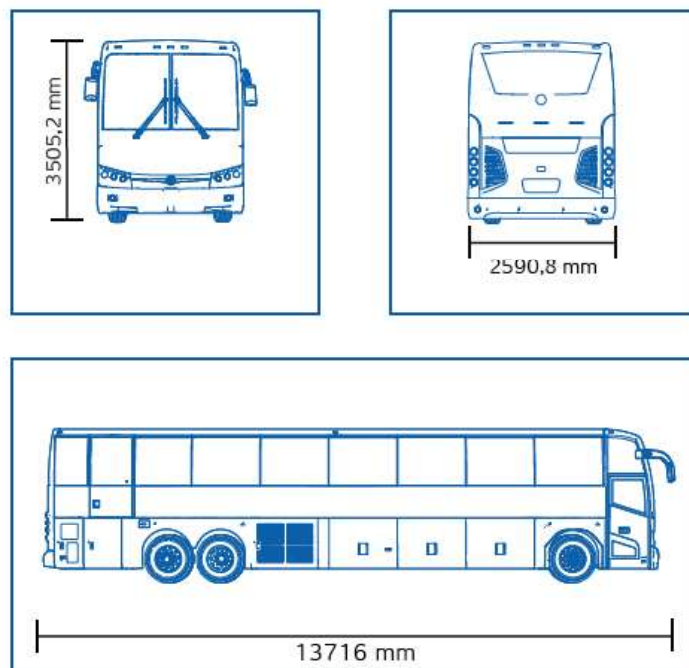
$$\dot{W}_{\text{rev}} = \dot{W}_{\text{comp}} - \dot{E}x_{\text{dest}} = \dot{E}x_{\text{out,comp}} - \dot{E}x_{\text{in,comp}} \quad (17)$$

where difference between minimum required power to be supplied to the compressor (useful work) is  $\dot{W}_{\text{comp}}$  and the exergy destruction is  $\dot{E}x_{\text{dest}}$ .

### 3. RESULTS AND DISCUSSION

Adana province of Turkey was chosen as the study region. In calculation of the cooling load of the inter-city bus cabin, climate data such as dry bulb temperature, wet bulb temperature and solar radiation of the Adana province were used. The selected bus, which has a passenger capacity of 56 persons, was used for inter-city passenger transportation in the United States and Turkey. Dimensions of the TS 45 type inter-city bus belonging to TEMSA are presented in Figure 2. Dry bulb temperature and wet bulb temperature of outdoor air was accepted as 36.8 °C and 25.7 °C, respectively. The inter-city bus cabin was maintained at 24.4 °C dry bulb temperature and 50% relative humidity. It was assumed that the inter-city bus was traveling to north direction at a speed of 120 km/h for the cooling load calculation.

Cooling Load Hourly Analysis Program (HAP) was used to determine hourly cooling load capacity of the intercity bus. Accordingly, maximum cooling load values were computed to be nearly 25-26 kW and obtained at 17:00, while the minimum values were acquired at times when atmospheric air temperature and solar radiation were low. Maximum cooling load value was obtained as 25.96 kW at 17:00 in July. It was also the peak cooling load and peak time. Therefore, the energy and exergy analysis of the inter-city bus AC system were made considering the calculated peak load values. The MR value was considered to be between 0.05 and 0.5. The inter-city bus cabin was considered at 24.4 °C dry bulb temperature and 50% relative humidity, while the outside design conditions were obtained 36.8 °C dry bulb temperature and 25.7 °C wet bulb temperature. The supplied air to the conditioned space was assumed to be 10 °C lower than the inside temperature, and thus determined as 14.4 °C.



Dimensions of inter-city bus in mm (TEMSA)					
Length	Width	Height	Wheelbase	Front Extension	Rear Extension
13716	2590.8	3505.2	7894.3	1925.3	1925.3
Inter-city bus engine (CUMMINS)					
Model	CUMMINS ISX EPA13 345 HP				
Type	Diesel				
Number of Cylinders	6 in line				

Figure 2. Dimensions of the TS 45 type inter-city bus [6]

The bus sensible cooling load ( $\dot{Q}_{\text{sensible,bus}}$ ) value and the bus latent cooling load value ( $\dot{Q}_{\text{latent,bus}}$ ) were determined as 22.808 kW and 3.154 kW. The thermodynamic properties of refrigerant R600a were determined using the CoolPack V2.85 software. In the calculations of the refrigeration cycle, value of the evaporation temperature of the refrigerant was considered to be equal to the apparatus dew point temperature. Condensation temperature of the refrigerant was considered to be 15 °C above the atmospheric air temperature. In addition, superheated and subcooling temperature values were defined as 10 °C. The dead-state temperature ( $T_0$ ) was considered to be environment temperature, 36.8 °C. The dead-state pressure ( $P_0$ ) was considered to be 101.325 kPa.

The effect of MR on COP values of the inter-city bus AC system and the compressor input powers is shown in Figure 3. Maximum useful work and reversible power values were obtained as 9.57 kW and 8.08 kW for MR=0.5, while minimum useful work and reversible power were found as 5.62 kW and 4.73 kW for MR=0.05, respectively. Determined COP values varied from 5.12 to 5.36, resulting in up to 4.6% difference. It was observed that useful work and reversible power increases significantly with increasing MR, thus resulting in reduction in COP.

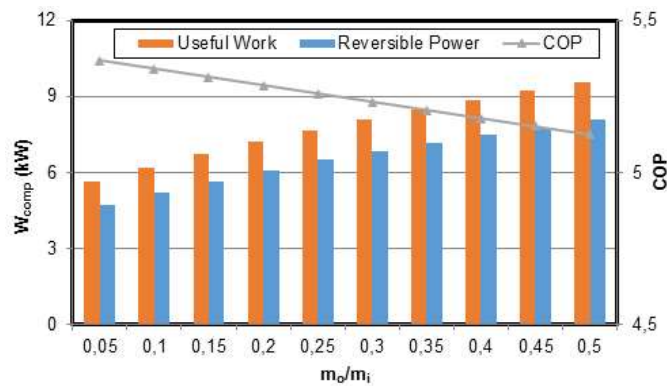


Figure 3. The effect of MR on COP values of the inter-city bus AC system and the compressor input powers

Figure 4 shows the heat transfer rates at condenser and evaporator with respect to MR. As seen from the figure, minimum heat transfer at condenser was observed as 35.79 kW at MR=0.05, while maximum heat transfer value was calculated as 58.59 kW at MR=0.5, causing 63.70% more energy consumption. On the other hand, minimum heat transfer at evaporator was 30.17 kW and obtained at MR=0.05, while maximum heat transfer at evaporator was 49.03 kW and obtained at MR=0.5, causing 62.51% more energy consumption. It is worthwhile to mention that increasing MR causes increment in the temperature and absolute humidity of air mixture. In this regard, it is the main reason for higher heat transfer rates.

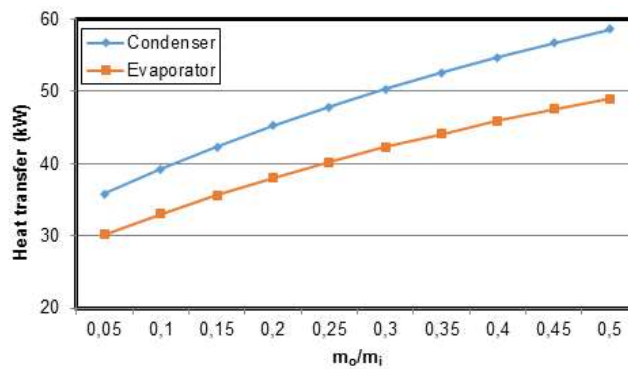


Figure 4. The heat transfer rates at condenser and evaporator with respect to MR

Figure 5 presents exergy destruction values of the inter-city bus AC system equipment with respect to MR for R600a. As presented in the figure, exergy destruction values of each system equipment increases with increasing MR. Maximum exergy destruction values of evaporator, condenser, compressor and expansion valve at MR=0.5 are 2.75 kW, 1.87 kW, 1.48 kW and 0.89 kW, while minimum exergy destruction values of these components at MR=0.05 are 1.15 kW, 1.32 kW, 0.88 kW and 0.51 kW, respectively.

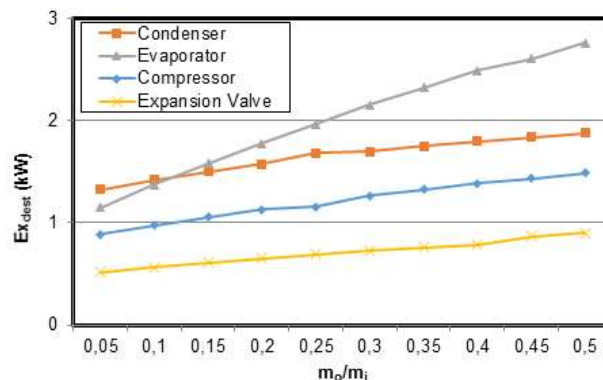


Figure 5. Exergy destruction values of the inter-city bus AC system equipment with respect to MR

Figure 6 shows exergy efficiency values of the inter-city bus AC system equipment with respect to MR. As demonstrated in the figure, exergy efficiency values of the each system component varies indistinctly with respect to MR. Exergy efficiencies of expansion valve, compressor, evaporator and condenser at MR=0.5 are 92.05%, 84.46%, 74.16% and 31.43%, whereas exergy efficiencies values at MR=0.05 are 92.52%, 84.18%, 83.36% and 19.64%, respectively. It is observed that expansion valve has the highest exergy efficiency values and condenser has the lowest exergy efficiency values for all MR values.

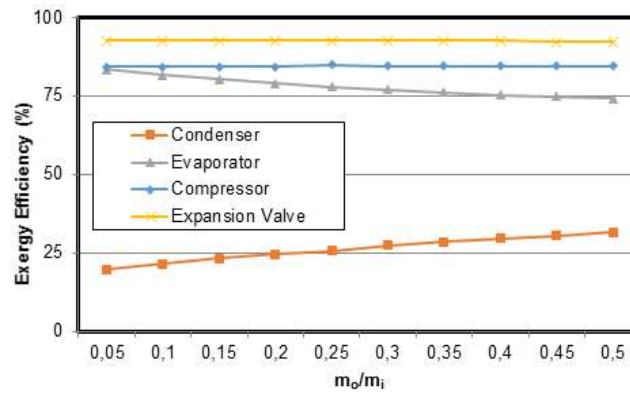


Figure 6. Exergy efficiency values of the inter-city bus AC system equipment with respect to MR

Figure 7 presents overall exergy efficiency and total exergy destruction values of the inter-city bus AC system with respect to MR for R600a. As can be observed from the figure, total exergy destruction values increase significantly in parallel with MR values, while overall exergy efficiency values do not change excessively. Maximum overall exergy efficiency and total exergy destruction are 46.45% and 7.02 kW, and minimum overall exergy efficiency and total exergy destruction are 45.67% and 3.88 kW, respectively.

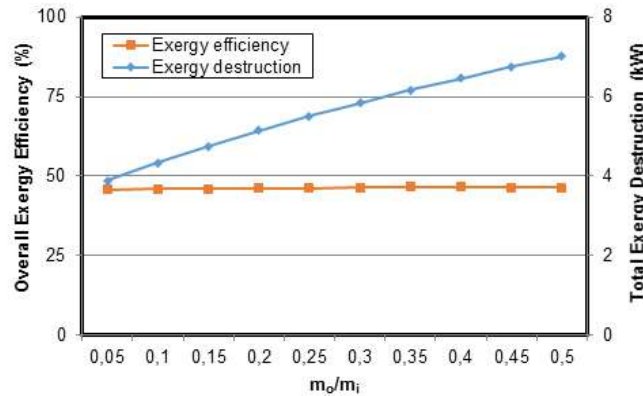


Figure 7. Overall exergy efficiency and total exergy destruction values of the inter-city bus AC system with respect to MR

#### 4. CONCLUSIONS

- Total exergy destruction values increase significantly in parallel with MR values,
- Maximum useful work and reversible power values were obtained as 9.57 kW and 8.08 kW for MR=0.5, while minimum useful work and reversible power were found as 5.62 kW and 4.73 kW for MR=0.05, respectively.
- According to the results for MR=0.5, exergy destruction values of the inter-city bus AC system were calculated to be 1.5 kW, 1.88 kW, 0.90 kW and 2.76 kW for the compressor, condenser, expansion valve and evaporator, respectively.
- Also, exergy efficiency values in these components were respectively found as 84.46%, 31.43%, 74.16% and 92.05%.
- Total exergy destruction and overall exergy efficiency of the system were obtained as 46.45% and 7.02 kW, respectively.

#### ACKNOWLEDGEMENTS

The authors would like to thank to TEMSA Global for its contribution.

#### REFERENCES

- [1] Bilgili, M., Ozbek, A., Sahin, B., Kahraman, A. (2015). An overview of renewable electric power capacity and progress in new technologies in the World. *Renewable and Sustainable Energy Reviews*, vol. 49, p. 323-334, DOI: 10.1016/j.rser.2015.04.148.

- [2] Chu, C.M., Jong, T.L. (2008). Enthalpy estimation for thermal comfort and energy saving in air conditioning system. *Energy Conversion and Management*, vol. 49, no. 6, p. 1620-1628, DOI: 10.1016/j.enconman.2007.12.012.
- [3] Weilenmann, M.F., Alvarez, R., Keller, M. (2010). Fuel consumption and CO<sub>2</sub> pollutant emissions of mobile air conditioning at fleet level-new data and model comparison. *Environmental Science and Technology*, vol. 44, no. 13, p. 5277-5282, DOI: 10.1021/es903654t.
- [4] Tosun, E., Bilgili, M., Tuccar, G., Yasar, A., Aydin, K. (2016). Exergy analysis of an inter-city bus air-conditioning system. *International Journal of Exergy*, vol. 20, no. 4, p. 445-464, DOI: 10.1504/IJEX.2016.078094.
- [5] Hurdogan, E., Buyukalaca, O., Hepbasli, A., Yilmaz, T. (2011). Exergetic modeling and experimental performance assessment of a novel desiccant cooling system. *Energy and Buildings*, vol. 43, no. 6, p. 1489-1498, DOI: 10.1016/j.enbuild.2011.02.016.
- [6] TEMSA. (2016). TS45 - Training Document (Vol. 1). Adana: Temsa Ulaşım Araçları Sanayi ve Ticaret A.Ş.